

Characterization of Magnetostrictive Iron-Gallium Alloys Under Dynamic Conditions

Undergraduate Honors Thesis

Presented in Partial Fulfillment of the Requirements for

Graduation with Distinction

at The Ohio State University

By

Craig Poeppelman

* * * * *

The Ohio State University

2010

Defense Committee:

Professor Marcelo Dapino, Advisor

Professor Yann Guezennec

Copyrighted by

Craig Poeppelman

2010

ABSTRACT

Galfenol alloys ($\text{Fe}_{1-x}\text{Ga}_x$) are a class of smart materials with favorable magnetostriction ($300 \mu\epsilon$) and mechanical robustness. Previous research has focused on static characterization of the material, but proposed applications operate in dynamic environments. In this work, a magnetomechanical transducer has been designed and constructed to conduct measurements of Galfenol samples 0.25 inches in diameter and 2.9 inches in length. The transducer was developed to conduct actuation and sensing measurements at both static and dynamic conditions. The corresponding measurement system was developed. This system has the ability to drive and measure the electrical, mechanical, and magnetic parameters of the system for both actuating and sensing measurements. Quasi static tests were conducted to verify the effectiveness of the transducer and measurement system. Dynamic actuation tests were also completed as a first step to characterizing Galfenol under dynamic conditions.

ACKNOWLEDGMENTS

I would like to thank all the people that have helped and supported me over the course of this project. I am thankful for the guidance provided by my advisor, Professor Marcelo J. Dapino. I would like to thank all the students and resources in the Smart Materials and Structures Lab, especially Phillip Evans and Arjun Mahadevan. This project would not have been possible without the support of the Department of Mechanical Engineering's facilities and the guidance of Joe West in the electronics shop.

TABLE OF CONTENTS

	<u>Page</u>
ABSTRACT.....	ii
ACKNOWLEDGMENTS	iii
TABLE OF CONTENTS.....	iv
LIST OF FIGURES	vi
Chapter 1: Introduction	1
1.1 Background.....	1
1.2 Literature Review	4
1.2.1 Magnetostrictive fundamentals.....	4
1.2.2 Static Galfenol characterization	5
1.2.3 Dynamic Galfenol characterization	8
1.2.4 Dynamic Terfenol-D research.....	9
1.3 Motivation.....	10
1.4 Project Objective	10
Chapter 2: Magnetomechanical Transducer	11
2.1 Design overview	11
2.2 Galfenol sample description	14
2.3 Circuit design.....	14
2.4 Steel laminates	15
2.5 Excitation coils	16
Chapter 3: Experiments.....	22
3.1 Measurement system overview.....	22
3.1.1 Inverse effect (actuation) measurements.....	25
3.1.2 Direct effect (sensing) measurements	27
3.2 Electrical system	28
3.3 Mechanical system.....	29
3.4 Magnetic system	29

Chapter 4: Results and Analysis	34
4.1 Quasi static actuation test	34
4.2 Mechanical model.....	36
4.3 Dynamic actuation tests.....	39
Chapter 5: Summary and Conclusions.....	45
BIBLIOGRAPHY	47
APPENDIX.....	49
Appendix A: Time domain plots of actuation tests	50
Appendix B: Signal filtering in actuation tests.....	59

LIST OF FIGURES

<u>Figure</u>	<u>Page</u>
Figure 1: Major magnetization loops of research grade Fe-Ga from (a) applied field with constant stress levels of 0, -9, -16, -23, -28, -32, -37, -42, -46 MPa and (b) applied stress with constant field levels of 1.9, 4.2, 2.4, 3.2, 4.8, 5.6, 6.5, 7.3, 8.1, 8.9 kA/m [9].	7
Figure 2: Magnetic induction and magnetostriction measurements of $\text{Fe}_{81.6}\text{Ga}_{18.4}$ Galfenol at stress levels of -1.38, -13.8, -41.4, -55.2, -69 MPa [8].	7
Figure 3: Magnetomechanical transducer designed and constructed for actuation and sensing tests of 18.4 at. % Ga and 20.9 at.% Ga samples.	13
Figure 4: Schematic of the magnetic flux traveling through the magnetomechanical transducer during an actuation test.	13
Figure 5: Research grade, polycrystalline $\text{Fe}_{81.6}\text{Ga}_{18.4}$ sample from Etrema Products.	14
Figure 6: 2D COMSOL simulation of the flux density through the proposed transducer conducted by a fellow grad student in the SMSL.	15
Figure 7: Image of stacked steel laminate pieces making up one half of flux return path in the transducer.	16
Figure 8: (a) A schematic of the constructed electromechanical transducer and (b) the transducer modeled as a magnetic circuit	17
Figure 9: Calibration of excitation coils used in the magnetomechanical transducer. Gains were calculated to be 36.1 (kA/m)/A and 36.9 (kA/m)/A respectively.	21
Figure 10: Overview of measurements for electrical, mechanical, and magnetic systems.	24
Figure 11: Diagram of an inverse effect (actuation) measurement.	26

Figure 12: Schematic of actuation measurements with (a) a mass load or (b) a prestress load.....	26
Figure 13: Diagram of a direct effect (sensing) measurement.....	27
Figure 14: Image of a direct effect (sensing) measurement.....	28
Figure 15: Schematic of electrical system including a line matching transformer to decouple the linear amplifier from the transducer.	29
Figure 16: Magnetization curves of Nickel 200 in the magnetomechanical transducer used to calibrate the MF-5D Fluxmeter for future testing.	32
Figure 17: Magnetization curves of Nickel 200 measured experimentally [12].	33
Figure 18: Quasi static actuation measurements of $\text{Fe}_{81.6}\text{Ga}_{18.4}$ sample conducted at 100 mHz.....	35
Figure 19: (a) Single degree of freedom mechanical model of Galfenol sample, m, subjected to a sinusoidal magnetic input, H, and (b) a free body diagram of the equivalent system.....	37
Figure 20: Frequency response of single degree of freedom mechanical model of Galfenol sample subjected to a sinusoidal magnetic input. The magnitude of the response is normalized such that the magnitude at 100 Hz is 0 dB.....	38
Figure 21: Magnetostriction-field curves for actuation measurements of $\text{Fe}_{81.6}\text{Ga}_{18.4}$ sample with a mass load of 50 lb at 1, 5, 10, 25, 50, 100, 200, 300, and 500 Hz. The minimum magnetostriction value was normalized to zero for each test.....	41
Figure 22: Magnetization-field curves for actuation measurements of $\text{Fe}_{81.6}\text{Ga}_{18.4}$ sample with a mass load of 50 lb at 1, 5, 10, 25, 50, 100, 200, 300, and 500 Hz. Magnetization values are normalized such that $M = 420 \text{ kA/m}$ at $H = 2 \text{ kA/m}$ at 1 Hz.....	42
Figure 23: Piezomagnetic constant, d, versus magnetic field for actuating measurements of $\text{Fe}_{81.6}\text{Ga}_{18.4}$ sample with a mass load of 50 lb at 1, 5, 10, 25, 50, 100, 200, 300, and 500 Hz. The values of d were calculated using numerical differentiation and filtered using a moving average. Values were calculated from $H = 1.3\text{-}2.7 \text{ kA/m}$ to avoid differentiation at the limits of the measurements.....	43
Figure 24: Susceptibility, $(\mu-1)$, versus magnetic field for actuating measurements of $\text{Fe}_{81.6}\text{Ga}_{18.4}$ sample with a mass load of 50 lb at 1, 5, 10, 25, 50, 100, 200, 300, and 500 Hz. Susceptibility values were calculated using numerical differentiation and	

filtered using a moving average. Values were calculated from $H = 1.3\text{-}2.7\text{ kA/m}$ to avoid differentiation at the limits of the measurements..... 44

CHAPTER 1

INTRODUCTION

1.1 Background

Today, development of innovative materials will be critical to the advancement of sensor and actuator technology. Advanced materials will be needed to push the aerospace industry to new heights, advance automotive technology to create safer and more efficient cars, and develop new breakthroughs in medical devices. Science has achieved significant advancements in technology with standard materials such as steel or aluminum that do not exhibit particularly special properties. The possibilities are endless for special materials that have adaptive properties to be manipulated to specific applications. These special materials, known as smart materials, are an area of study that can bridge the gap between today's technology and tomorrow's innovations.

Smart materials are defined to have one or more properties that significantly change in a controlled fashion based on external conditions such as temperature, stress, electric field, and magnetic field. This behavior enables them to transduce energy from one form to another efficiently. These properties have made smart materials promising to use both as actuators and sensors. Traditionally, shape memory alloys (SMA) and piezoelectric materials have been the most researched smart materials. SMA behavior

makes them suited for high strain, low bandwidth applications. On the contrary, piezoelectric materials are used for applications with low strain and high bandwidth [1].

Magnetostrictive materials, a subset of smart materials, are distinguished by their ability to change dimensional shape from an applied magnetic field as well as produce a magnetic field from an applied stress. These properties encourage the development of magnetostrictive materials for use in actuators and sensors in industrial, biomedical, and defense applications. Devices could be more compact, responsive, and require less moving parts than conventional technologies. Examples of magnetostrictive actuators include active vibration control, sonar transducers, and micropositioners. Examples of sensors include noncontact torque sensors, wave guide position sensors, and acoustic sensors [2].

The study of magnetostrictive materials was started by James P. Joule in 1842 when he first observed that a sample of iron changes in length when magnetized by a magnetic field. Subsequent work began with ferromagnetic materials, such as nickel, cobalt, and iron, which exhibited magnetostriction on the order of 10×10^{-6} . These materials and their alloys led to early applications including telephone receivers, hydrophones, scanning sonar, fog horns, and torque sensors. A breakthrough in magnetostrictive materials occurred in 1963 when it was discovered that rare earth elements terbium and dysprosium exhibited magnetostrictions on the order of $10,000 \times 10^{-6}$. Search began in the 1970's for an alloy that exhibited great magnetostriction utilizing these rare earth elements at room temperature, had reasonable

saturation, and had favorable mechanical properties. Development of the compound $\text{Tb}_{0.3}\text{Dy}_{0.7}\text{Fe}_{1.9-1.95}$ revealed magnetostriction values of $1,600 \times 10^{-6}$ at room temperature at a moderate saturation field of 160 kA/m. This product has been commercially available since the 1980's under the name Terfenol-D [4]. Great interest in Terfenol-D remains due to its high magnetostriction values compared to ferromagnetic materials, but widespread application of it is restricted by its poor mechanical properties.

Recently, the search for a mechanically robust magnetostrictive material has led to the development of Galfenol alloys ($\text{Fe}_{1-x}\text{Ga}_x$). This material, initially developed by the Naval Ordnance Laboratory, possesses superior characteristics compared to other magnetostrictive materials. Galfenol alloys exhibit moderate magnetostriction while still maintaining the mechanical robustness of steel by showing the ability to handle compressive, tensile, bending, torque, and shock loads. With its unique metallurgical and mechanical properties, it has the potential to enable smart load bearing devices and structures manufactured by extrusion, rolling, deposition, welding, or machining. Possible applications of Galfenol alloys include nanoacoustic sensors that mimic the cilia of the inner ear, sonar transducers with load-bearing properties, and shock-tolerant adaptive structures [7]. These promising characteristics make Galfenol an ideal material for developing smarter actuators and sensors, but more work needs to be completed to understand its behavior.

1.2 Literature Review

1.2.1 Magnetostrictive fundamentals

Magnetostrictive materials are characterized by the coupling between magnetic and mechanical domain. The magnetization \mathbf{M} , or flux density $\mathbf{B} = \mu_0(\mathbf{H} + \mathbf{M})$, and the response of strain \mathbf{S} to magnetic field \mathbf{H} and stress \mathbf{T} is nonlinear and depends on material history. The major components of the nonlinear behavior are saturation and anisotropy. Saturation occurs due to both magnetization and magnetostriction. Magnetostrictives are directionally dependent, anisotropic, in that they will not exhibit the same magnetostriction in one crystal direction as opposed to another.

To avoid the complex nonlinear behavior, transducers are often designed to operate in small operating ranges about a bias field and stress. The constitutive behavior can be expressed by piezomagnetic equations,

$$\mathbf{B} = \boldsymbol{\mu}^T \mathbf{H} + \mathbf{d} \mathbf{T}, \quad (1.1)$$

$$\mathbf{S} = \mathbf{d}^T \mathbf{H} + \mathbf{s}^H \mathbf{T}. \quad (1.2)$$

The equations contain the following coupling coefficients: the permeability tensor $\boldsymbol{\mu}^T$, the compliance tensor \mathbf{s}^H , and the piezomagnetic tensor \mathbf{d} . The piezomagnetic tensor \mathbf{d} determines the maximum available strain or free strain which occurs under the mechanically free condition which $\mathbf{T} = 0$. The free strain is $\mathbf{d}^T \mathbf{H}$. The piezomagnetic tensor and the compliance tensor determine the maximum possible stress which occurs when $\mathbf{S} = 0$. The blocked stress is $(\mathbf{s}^H)^{-1} \mathbf{d} \mathbf{H}$.

The energy density or work capacity is half the product of free strain and blocked stress. The free energy G is shown by the following equation,

$$G = \frac{1}{2}(\mathbf{T} \cdot \mathbf{S} + \mathbf{H} \cdot \mathbf{B}) \quad (1.3)$$

$$= \frac{1}{2}\mathbf{T} \cdot \mathbf{s}^H \mathbf{T} + \frac{1}{2}(\mathbf{T} \cdot \mathbf{d}^T \mathbf{H} + \mathbf{H} \cdot \mathbf{d} \mathbf{T}) + \frac{1}{2}\mathbf{H} \cdot \boldsymbol{\mu}^T \mathbf{H} \quad (1.4)$$

$$= G_{mechanical} + 2G_{coupling} + G_{magnetic} \quad (1.5)$$

The coupling coefficient k quantifies the efficiency of transduction which can be characterized by the following equations,

$$k = \frac{G_{coupling}}{\sqrt{G_{mechanical}G_{magnetic}}}, \quad (1.6)$$

$$k = \frac{\mathbf{d}^2}{\mathbf{s}^H \boldsymbol{\mu}^T} \quad (1.7)$$

These coupled equations define the behavior of magnetostrictive transducers. The coupling coefficients are important material properties needed when designing these devices [1], [6].

1.2.2 Static Galfenol characterization

Previous work has been completed modeling and measuring the quasi static characterization of Galfenol. This work was completed to understand the nonlinear and hysteretic magnetization as well as the magnetomechanical coupling. Kellogg et al. conducted various quasi static tests with both single crystal and polycrystalline samples of $\text{Fe}_{81}\text{Ga}_{19}$. It was found that the field required to saturate the samples was low, 400 Oe, for varying compressive stresses up to 87.1 MPa. As the compressive stress in the

sample increases, so does the magnetostriction but larger fields are necessary to produce saturation. The samples also exhibited temperature insensitive behavior. The material exhibited only a small reduction, 12%, in magnetostriction as the temperature increased from -21°C to 80°C. The maximum magnetostriction observed was 340×10^{-6} and 320×10^{-6} at room temperature. Various polycrystalline samples were also tested. The magnetostriction was observed to be much lower than single crystal samples, 170×10^{-6} . Despite the lower values for polycrystalline samples, large magnetostriction at moderate field levels confirmed Galfenol's suitability for actuators and sensors [10].

Additional work was completed by Evans and Dapino measuring production and research grade Galfenol samples under quasi static conditions. A production grade sample, $\text{Fe}_{81.6}\text{Ga}_{18.4}$, and a research grade sample, $\text{Fe}_{81.5}\text{Ga}_{18.5}$, were measured by comparing a series of applied field at constant stress and applied stress at constant field experiments. From these tests, a high degree of reversibility was observed in both samples. Results from the tests are shown below in Figure 1 and Figure 2. In addition to measurements, a constitutive model relating magnetization and strain to magnetic field and stress was developed through thermodynamic principles with stochastic homogenization. It is expected that the model will accurately simulate the behavior of Galfenol once densities are optimized [9].

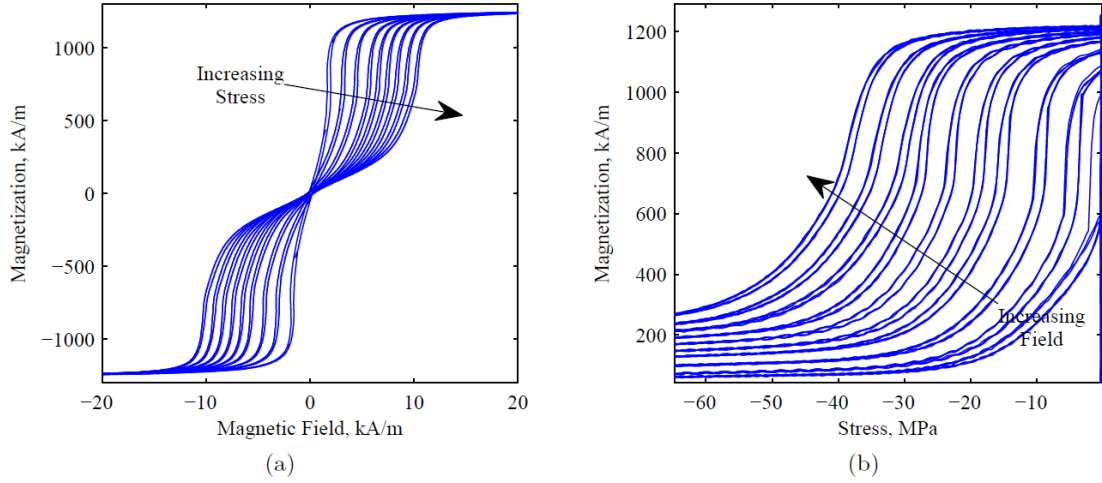


Figure 1: Major magnetization loops of research grade Fe-Ga from (a) applied field with constant stress levels of 0, -9, -16, -23, -28, -32, -37, -42, -46 MPa and (b) applied stress with constant field levels of 1.9, 4.2, 2.4, 3.2, 4.8, 5.6, 6.5, 7.3, 8.1, 8.9 kA/m [9].

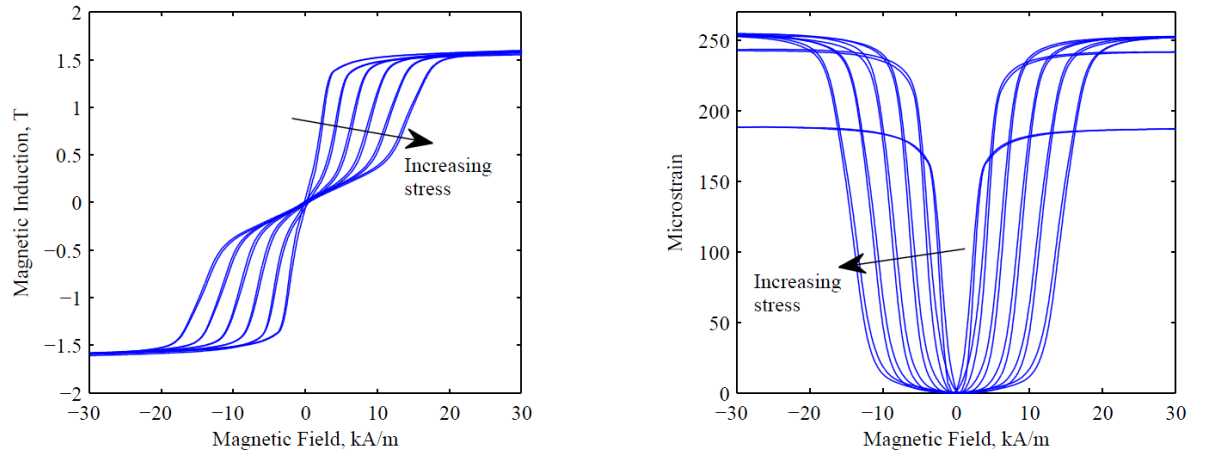


Figure 2: Magnetic induction and magnetostriction measurements of Fe_{81.6}Ga_{18.4} Galfenol at stress levels of -1.38, -13.8, -41.4, -55.2, -69 MPa [8].

1.2.3 Dynamic Galfenol characterization

As mentioned earlier, much of the investigation in Galfenol has focused on quasi static characterization. There has been work characterizing the material under dynamic conditions. Evans and Dapino have developed a fully coupled magnetoelastic model of Galfenol incorporating eddy current losses and thermal relaxation. In a magnetic material, a changing magnetic induction \mathbf{B} creates an electric field \mathbf{E} which finally creates a magnetic field \mathbf{H} opposing the changing magnetic induction. These dynamic losses due to eddy currents can be described by Maxwell's equations,

$$\nabla \times \mathbf{E} = -\frac{\partial \mathbf{B}}{\partial t}, \quad (1.8)$$

$$\mathbf{J} = \frac{1}{\rho_e} \mathbf{E}, \quad (1.9)$$

$$\nabla \times \mathbf{H} = \mathbf{J}. \quad (1.10)$$

Losses due to eddy currents will occur in magnetostrictive materials when a time varying stress \mathbf{T} is applied or a time varying magnetic field \mathbf{H} . The dynamic model was used to simulate a theoretical Tonpilz transducer composed of Galfenol rod in a closed magnetic circuit. Actuating and sensing simulations at 100 Hz show the effect of eddy currents on the transducer's response [8].

In addition to dynamic modeling, work has been completed by Twarek and Flatau measuring Galfenol's response under dynamic conditions. Tests were conducted with single crystal cylindrical Galfenol rods, $\text{Fe}_{77.5-82}\text{Ga}_{18-22.5}$. Tests were completed with both solid and laminated samples to compare the effects of eddy currents on the efficiency of transduction. The study showed that the magnetomechanical coupling coefficient

increased by ~50% for the laminated rod compared to the solid rod. These tests were a valuable start to the dynamic characterization of Galfenol, but much more still needs to be investigated [13].

1.2.4 Dynamic Terfenol-D research

Unlike Galfenol, significant research has been conducted on the dynamic characterization of Terfenol-D. Calkins, Dapino, and Flatau investigated its material properties at various frequencies. First, a study on the effect of prestress on Terfenol-D's dynamic performance. Dynamic tests revealed a large reduction in the strain versus applied field slope in dynamic tests compared with static tests. The study helped identify optimal prestress and magnetic bias which to optimize the coupling and axial strain coefficient at various frequencies [3]. Another investigation studied Terfenol-D's properties under various conditions using a statistical study. The study showed a variance smaller than 5% between samples at the same experimental conditions. The results of the investigation emphasized the importance of adequate sampling in magnetostrictive transducer studies [5]. Investigations similar to this for Galfenol would be invaluable to its characterization and accelerate its development to real world applications.

1.3 Motivation

From the literature review, established modeling and testing has been completed with Galfenol. This work has been primarily focused on studying its behavior in static conditions, but many possible applications would operate at dynamic conditions. Therefore, this project aims to characterize the behavior under dynamic conditions. This investigation will be important to correlate with other scientists working on Galfenol as part of a MURI grant through the Office of Naval Research. Advances in studying Galfenol's dynamic behavior will be part of an effort to create a software module fully characterizing its properties. This module is important for the end user trying to control Galfenol devices.

1.4 Project Objective

The objective of this project is to advance the investigation of Galfenol's behavior under dynamic conditions. Material properties to be investigated include the interaction between the mechanical and magnetic responses. A magnetomechanical transducer will be designed and built to gather necessary data. A measurement system with appropriate sensors and data acquisition will be developed. Quasi static measurements will be made to validate this transducer and behavior of the samples used in this study. Finally, dynamic tests will be conducted to characterize the transducer and Galfenol.

CHAPTER 2

MAGNETOMECHANICAL TRANSDUCER

In this section the magnetomechanical transducer designed and constructed for this project is discussed. The transducer was designed to measure the direct (sensing) and inverse (actuation) effect of a research grade, highly textured, $\langle 100 \rangle$ oriented polycrystalline Galfenol alloy with a composition of $\text{Fe}_{81.6}\text{Ga}_{18.4}$. The system could be operated in both static or dynamic conditions, as previous research in Galfenol has been limited for the most part to static measurements.

2.1 Design overview

A primary focus of this project was to design and construct a magnetomechanical transducer to be used for sensing and actuation measurements in both static and dynamic conditions. The transducer needed to be designed to satisfy certain assumptions of the system: uniform strain and magnetic field along the length of a Galfenol rod. Also, the following properties needed to be measured: average magnetic flux density over the cross-section of the rod, total elongation, surface magnetic field, and applied force. Therefore, the device needed to have the functionality to couple with the necessary

testing equipment and measurement devices. An image of the constructed transducer can be seen below in Figure 3, and detailed analysis of its design follows in subsequent sections.

The transducer would act as a magnetic circuit, so magnetic flux could travel through the Galfenol samples studied. The magnetic circuit consists of two excitation coils connected in parallel and a flux return path made of steel laminates. The two coils were connected such that they were wound in opposite directions creating magnetic flux that flowed in opposite directions and into the Galfenol sample connected in parallel. A depiction of this magnetic flow is shown below in Figure 4.

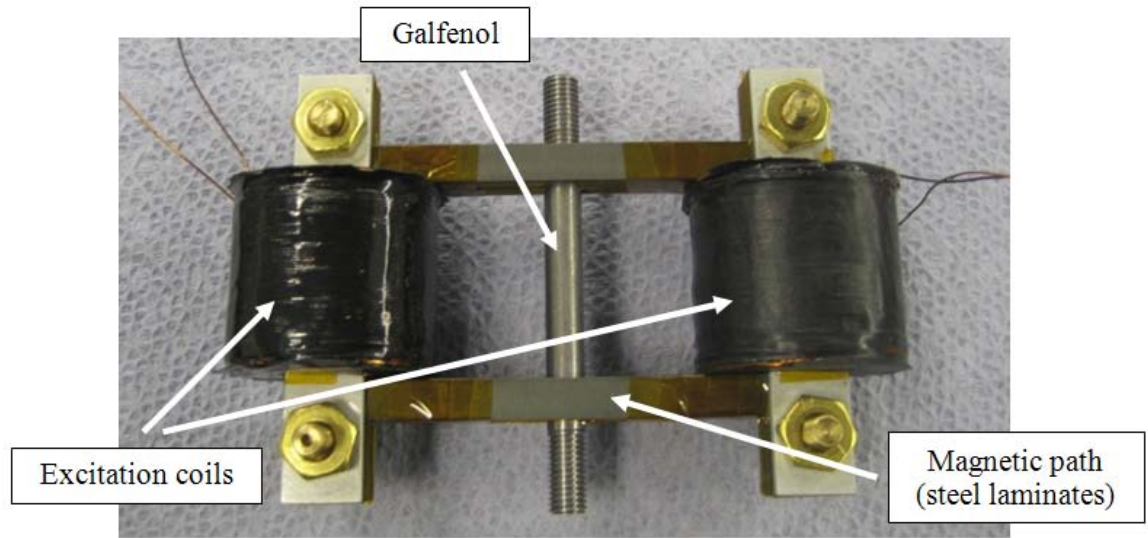


Figure 3: Magnetomechanical transducer designed and constructed for actuation and sensing tests of Galfenol rods.

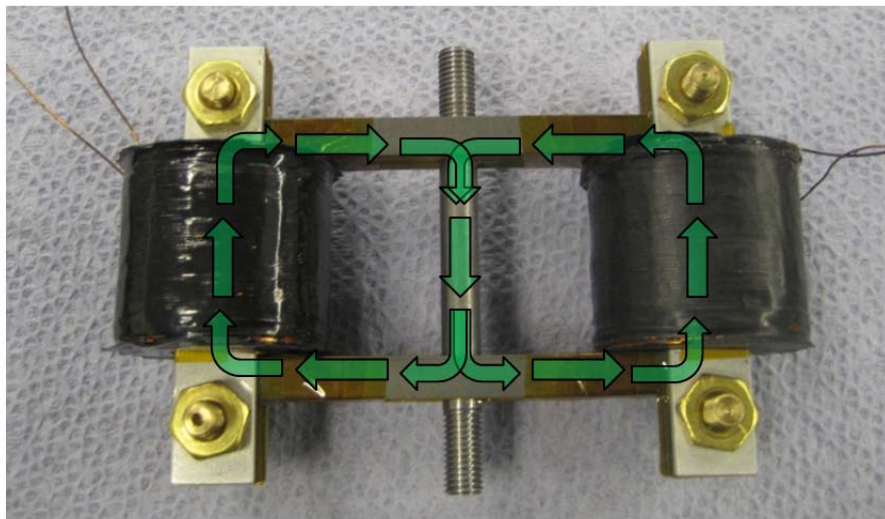


Figure 4: Schematic of the magnetic flux traveling through the magnetomechanical transducer during an actuation test.

2.2 Galfenol sample description

The iron-gallium alloys used for this study were purchased from Etrema Products. An image of the $\text{Fe}_{81.6}\text{Ga}_{18.4}$ sample is shown below in Figure 5. The sample measured 0.25 inches in diameter and 2.9 inches in length. The sample was grown by the FSZM method. The ends of the samples were threaded, 1/4 x 28, using standard HSS tools and traditional cutting procedures. The purpose of threading the ends was for the samples to couple with stainless steel end caps needed for connection to hydraulic press measurement systems.

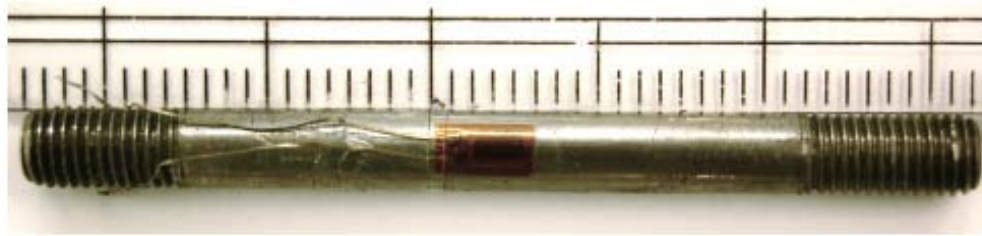


Figure 5: Research grade, polycrystalline $\text{Fe}_{81.6}\text{Ga}_{18.4}$ sample from Etrema Products.

2.3 Circuit design

Various designs to produce the necessary qualifications of the transducer were investigated. The goal was to design a magnetic circuit that produced a uniform magnetic flux along the length of the Galfenol sample while minimizing the magnetic flux decay. Two dimensional simulations were conducted by a fellow grad student in the

SMSL in the software package COMSOL. The simulations were used to quantify the uniformity of magnetic flux along the length of the Galfenol rod. The different designs utilized various geometries and means to connect the flux return path to minimize air gaps and flux leakage. The final design is shown below in 6.

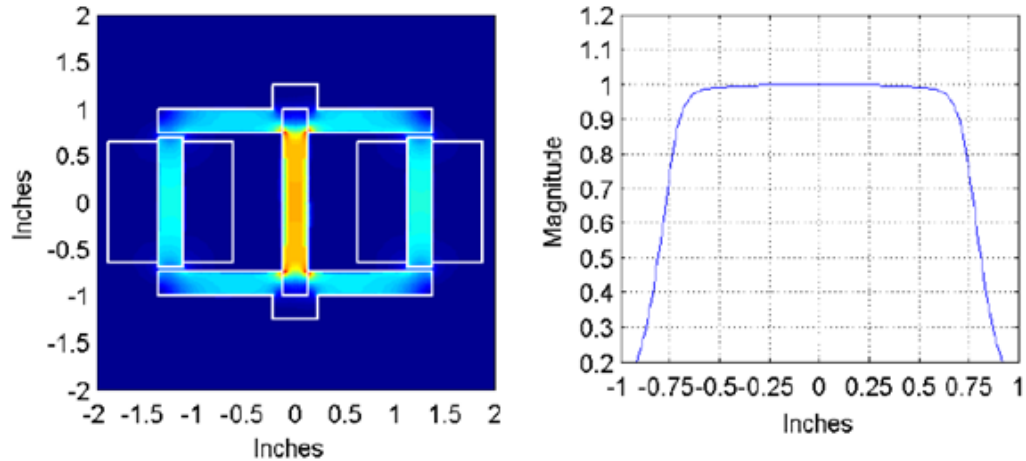


Figure 6: 2D COMSOL simulation of the flux density through the proposed transducer conducted by a fellow grad student in the SMSL.

2.4 Steel laminates

The magnetic circuit constructed consists of a steel flux return path. A concern with testing at higher frequencies is the prevalence of eddy current losses in the system. This loss was described previously in equations 1.8 to 1.10. To minimize the effect of eddy currents in the circuit, the steel of the transducer was laminated. Laminated plates

of steel reduce the cross section of the flux path decreasing the eddy currents for a given flux density.

The steel laminates in the transducer were constructed out of 0.018 inch thick sheets. Each laminate piece was laser cut to a precise geometry. Insulating tape was applied between each laminate, and twenty laminate pieces were stacked together to create each of the two major sections of the flux return path. The entire path was created in two sections to allow for easier assembly of the transducer. One section of the flux return path, one half of the total path, is shown below in Figure 7.

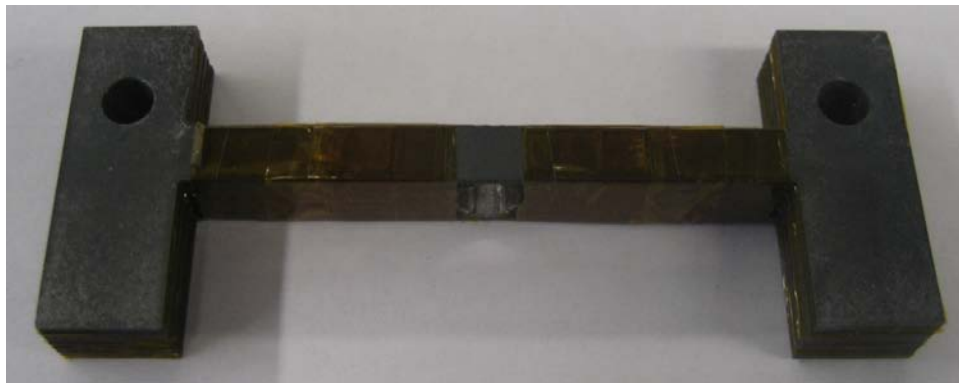
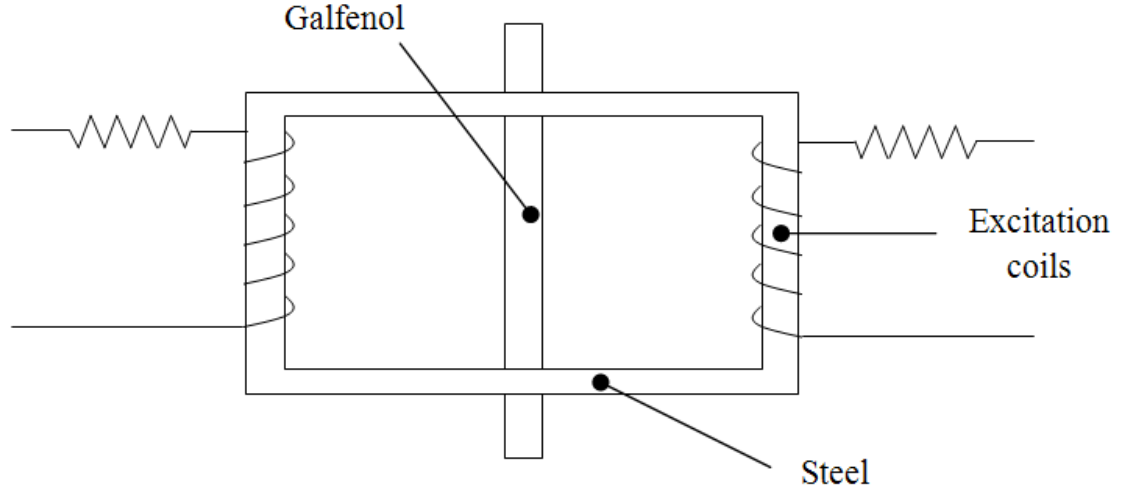


Figure 7: Image of stacked steel laminate pieces making up one half of flux return path in the transducer.

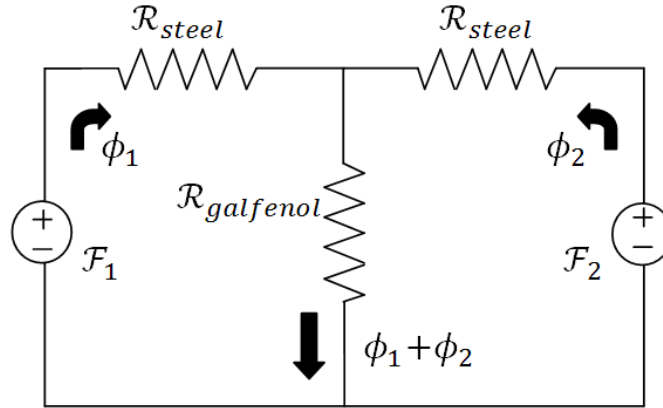
2.5 Excitation coils

Another important aspect of the transducer is the design of the excitation coils. These coils drive the system during actuation tests; therefore, the appropriate size of the coils is important to reach the saturation level of the Galfenol without requiring excess

current. It was assumed that a field of 30 kA/m through the Galfenol would be sufficient to saturate it in the stress range of interest. The current required to produce this field needed to be less than 1 ampere to ensure that the coils would not overheat during testing.



(a)



(b)

Figure 8: (a) A schematic of the constructed electromechanical transducer and (b) the transducer modeled as a magnetic circuit

To determine the required number of turns in the coils, the transducer was modeled as a magnetic circuit. A schematic of the transducer and its corresponding magnetic circuit are shown in Figure 8. To determine the required magneto motive force, \mathcal{F} , of each coil, Kirchhoff's voltage law is applied to the left and right loops of the circuit,

$$\mathcal{F}_1 - \phi_1 \mathcal{R}_s - (\phi_1 + \phi_2) \mathcal{R}_g = 0 , \quad (2.1)$$

$$\mathcal{F}_2 - \phi_2 \mathcal{R}_s - (\phi_1 + \phi_2) \mathcal{R}_g = 0 , \quad (2.2)$$

$$\phi_g = \phi_1 + \phi_2 . \quad (2.3)$$

Assuming that each excitation coil is driven equally and has the same gain, equation 2.1 can be simplified as follows,

$$\mathcal{F}_1 - \frac{\phi_g \mathcal{R}_s}{2} - \phi_g \mathcal{R}_g = 0 , \quad (2.4)$$

$$\mathcal{F}_1 = N_1 i_1 \quad (2.5)$$

$$\phi_g = \frac{2N_1 i_1}{\mathcal{R}_s + 2\mathcal{R}_g} . \quad (2.6)$$

Manipulating this equation to determine the number of turns in each coil, N_1 ,

$$H = \frac{\phi}{A\mu_r\mu_o} \quad (2.7)$$

$$N_1 = H(\mathcal{R}_s + 2\mathcal{R}_g)A\mu_r\mu_o \left(\frac{1}{i_1} \right) \quad (2.8)$$

\mathcal{R}_s and \mathcal{R}_g can be calculated from the geometry of the transducer. Equation 2.8 can be solved with the following values to determine the number of turns in each coil,

H	$30 \frac{\text{kA}}{\text{m}}$
\mathcal{R}_s	$2.03 \times 10^5 \text{ H}^{-1}$
\mathcal{R}_g	$3.01 \times 10^6 \text{ H}^{-1}$
A	$3.17 \times 10^{-5} \text{ m}^2$
μ_r	329
μ_o	$4\pi \times 10^{-7} \frac{\text{H}}{\text{m}}$
i_1	1 A .

Solving equation 2.8 yields the result,

$$N_1 = 1183 \text{ turns} \quad (2.9)$$

Based on this calculation and adding a safety factor, the coils were wound with approximately 1600 turns.

To construct the coils, an assembly was machined out of aluminum that included two end caps three inches in diameter connected by a rectangular cross section piece. This piece had the same dimensions as the steel laminates, 0.50 inches by 0.50 inches, to ensure the coils would mate tightly around the flux return path. This tolerance was kept low to minimize leakage in the magnetic circuit. The end caps were lined with a layer of insulating tape from Captain Inc. This layer of tape wrapped around the entire end cap to

ensure that the coil would bond to the tape and not the end cap. Next, one layer of fishing line was wrapped around the rectangular cross section piece. The coil was then wound by slowly wrapping #26 gage copper wire. To hold the coil in place, a layer of epoxy was applied between every other layer of wire.

The two finished coils each had a nominal resistance of 16 ohms, approximately 1600 turns, and a length of 1.2 inches. The gain of the coils was calibrated by measuring the resulting field inside each coil at varying currents using an HP245S longitudinal Hall probe and MJ-4D Gaussmeter from Walker Scientific. Figure 9 shows the calibration of each coil. The gains of the coils are 36.1 and 36.9 (kA/m)/A. With only a 2.0% difference in gains, uneven magnetic flux in each half of the transducer would be negligible.

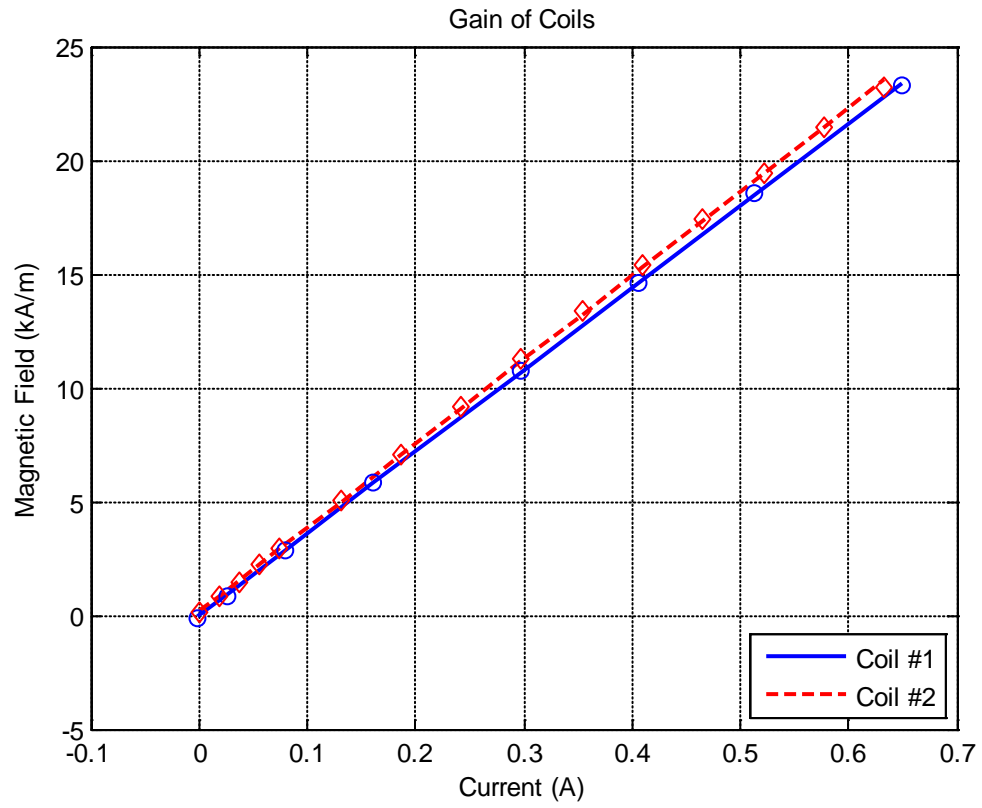


Figure 9: Calibration of excitation coils used in the magnetomechanical transducer. Gains were calculated to be 36.1 (kA/m)/A and 36.9 (kA/m)/A respectively.

CHAPTER 3

EXPERIMENTS

In this section, the measurement system developed to test Galfenol specimens in the designed transducer is discussed. The goal of this project is to characterize Galfenol under dynamic conditions, therefore a sufficient measurement system is needed to collect quality data at both low and high frequencies. The measurement system must be developed both for sensing and actuation tests. Electrical, mechanical, magnetic systems needed to be monitored in testing, and subsequent sections will discuss each section in more detail.

3.1 Measurement system overview

The experiments conducted needed to measure signals in the electrical, mechanical, and magnetic domains. The necessary parameters to be measured are shown below in Table 1 and a schematic of the complete measurement system is shown in Figure 10. The data acquisition device used for testing was a SignalCalc Quattro from Data Physics. It has 4 input channels as well as two output channels of $\pm 10V$ for

creating signals in actuation tests. The maximum sampling rate is 204.8 kHz which is more than adequate for the range of frequencies desired for testing.

Table 1: Measurements needed in experimental setup.

Electrical	Mechanical	Magnetic	Signal
Voltage V (V)	Stress σ (MPa)	Magnetic Field H (kA/m)	Frequency f (Hz)
Current A (mA)	Strain ϵ ($\mu\epsilon$)	Magnetization M (kA/m)	Waveform [sine, step]

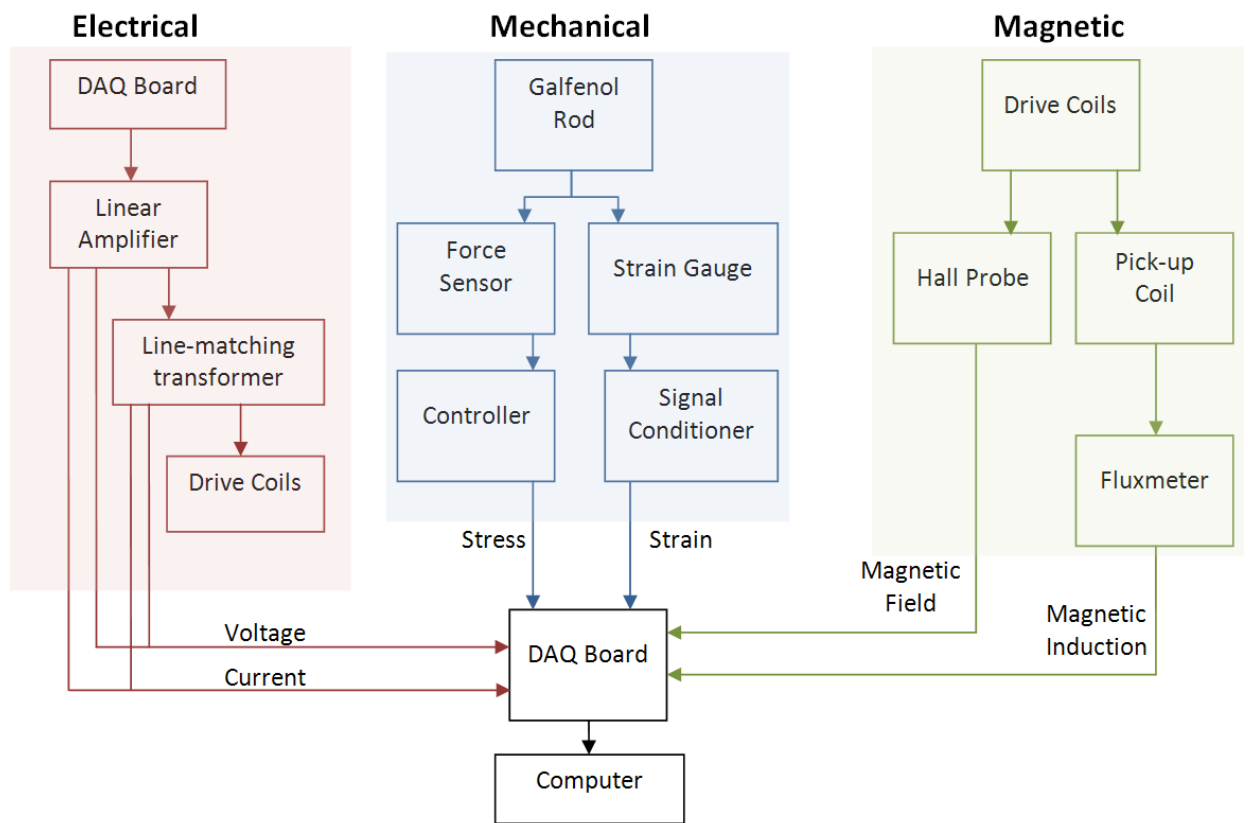


Figure 10: Overview of measurements for electrical, mechanical, and magnetic systems.

3.1.1 Inverse effect (actuation) measurements

The inverse effect of magnetostrictive materials is characterized by the material being subjected to a magnetic input and producing a mechanical output. A sinusoidal electrical signal generated by the data acquisition device is amplified and sent to the excitation coils. The coils create a magnetic flux through the closed magnetic circuit which flows through the Galfenol sample. This magnetic flux in the sample creates a mechanical output. A schematic of the test is shown below in Figure 11.

The magnetization versus field (M-H) and magnetostriction versus field (λ -H) measurements are to be monitored. To operate in the linear range of response, the sample is subjected to a magnetic bias which also enables the material to respond at the same frequency as the input. Without a magnetic bias, the Galfenol would exhibit a response at twice the frequency of the input. To create the magnetic bias, a DC offset is generated in the DAQ output signal sent to the amplifier. To calibrate this offset, quasi static measurements are conducted before the tests to determine the appropriate current to create the desired magnetic bias. A mechanical prestress can be applied to the system to increase the magnetostriction output based on the known characterization of Galfenol [8]. This prestress can be applied by a elastomer test frame or by Belleville spring washers. A mass load can be coupled to the system which will affect the mechanical system and therefore the response of the system. Schematics of a prestress and mass load setup are shown in Figure 12.

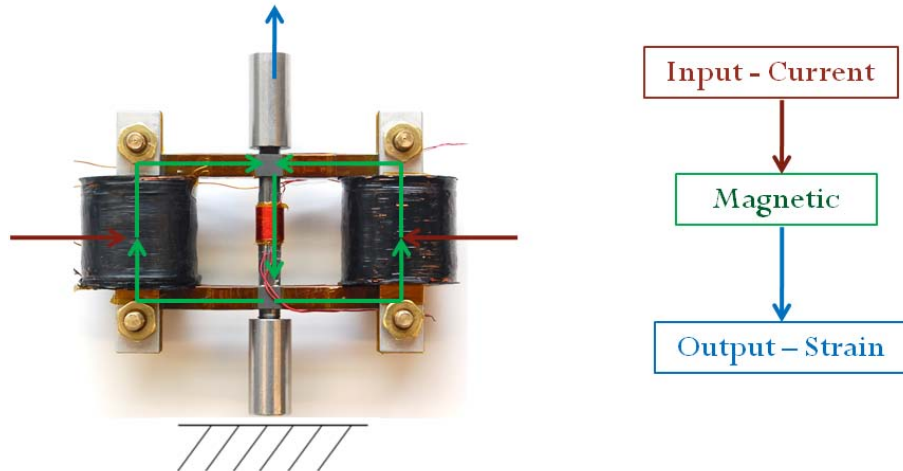


Figure 11: Diagram of an inverse effect (actuation) measurement.

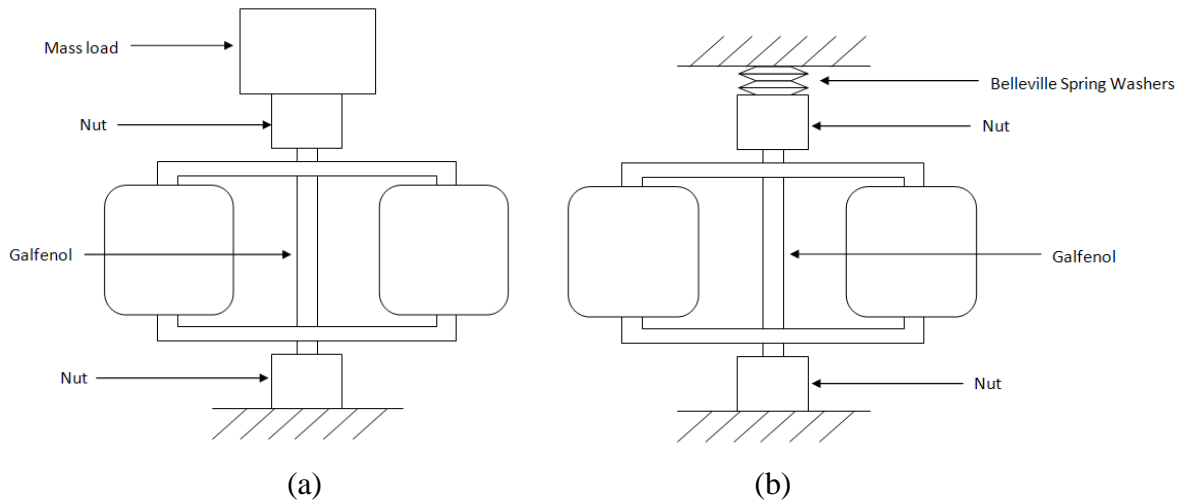


Figure 12: Schematic of actuation measurements with (a) a mass load or (b) a prestress load.

3.1.2 Direct effect (sensing) measurements

The direct effect of magnetostrictive materials is characterized by the material being subjected to a force input and producing a magnetic output. A stress input to the system is supplied by an elastomer test frame. The magnetic output is measured from the pick-up coil placed at the center of the Galfenol sample. A diagram of a sensing measurement is shown in Figure 13 and a photo of a sensing measurement is shown in Figure 14.

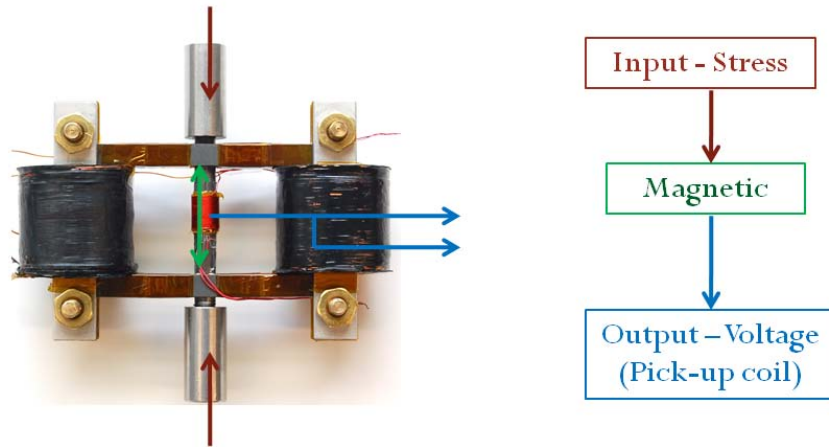


Figure 13: Diagram of a direct effect (sensing) measurement.

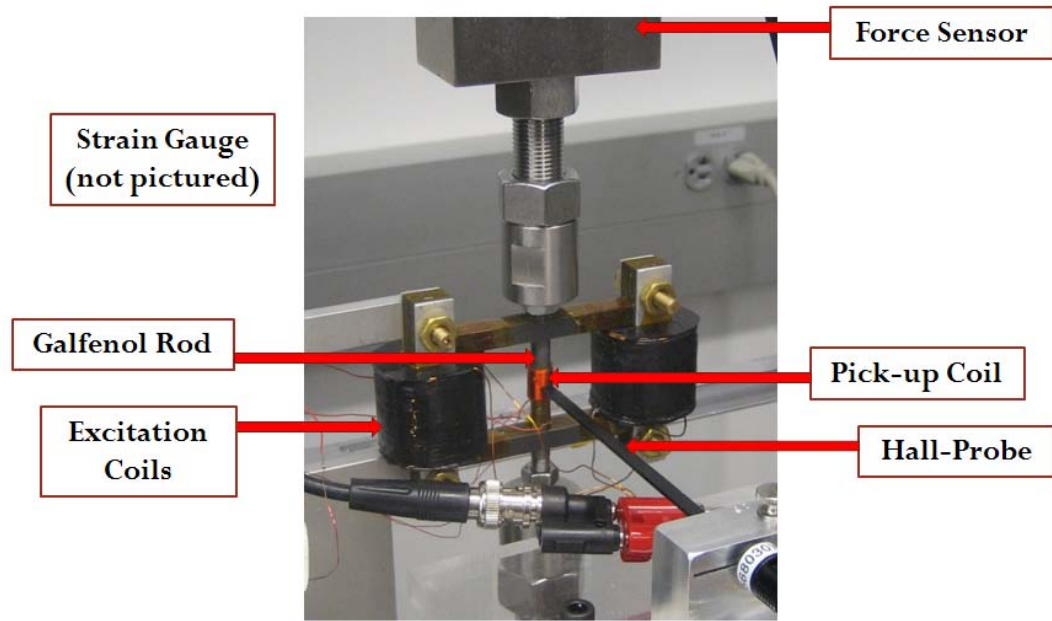


Figure 14: Image of a direct effect (sensing) measurement.

3.2 Electrical system

Power to the system originates from a signal created by the SignalCalc Quattro, sent to an AE Techron 5050 linear amplifier, and finally sent to the excitation coils of the transducer. The two excitation coils were connected in parallel and driven by the same source. The DC load of the system is 8 ohms. The voltage and current monitor of the amplifier were sent to the Quattro data acquisition system. At high frequencies, the load of the transducer becomes capacitive. Therefore, the amplifier's response to the system became unreliable. To combat this, an Atlas T18 line matching transformer was connected in parallel to the circuit to decouple the transducer load from the amplifier. A schematic of this system is shown below in Figure 15.

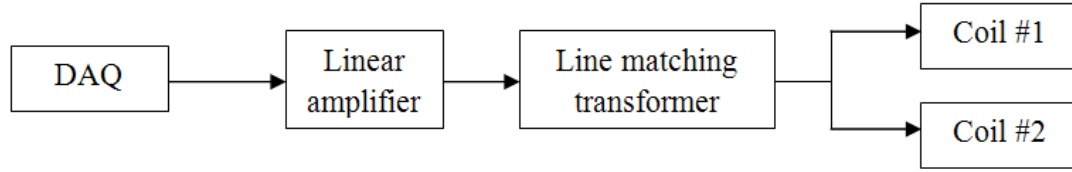


Figure 15: Schematic of electrical system including a line matching transformer to decouple the linear amplifier from the transducer.

3.3 Mechanical system

The two quantities to be measured in the mechanical domain are stress and strain. For stress, force sensors were used in elastomer test frames which were converted to stresses. To measure strain, an OMEGA (SGD-3/350-LY11) axial strain gage was bonded to the center of the Galfenol sample. The output from the strain gage was sent to a Vishay 2310 B signal conditioner. The outputs from the force sensor and signal conditioner were sent to the Quattro data acquisition system.

3.4 Magnetic system

For magnetic parameters, the magnetic field and flux density were measured at the center of the testing sample. Significant work was conducted to select appropriate sensors and calibrate them for each measurement. To measure field, an HP145S transverse Hall probe from Walker Scientific was stationed at the center of the test

sample perpendicular to its axial direction as seen in Figure 14. The Hall probe was connected to a MG-4D Gaussmeter from Walker Scientific. The Gaussmeter produces an analog output collected by the Quattro data acquisition device.

To measure the flux density, a pick-up coil was wound with 74 turns and an inside diameter of 0.25 inches. The pick-up coil was placed at the center of the test sample as seen in Figure 14. The voltage across the pick-up coil is collected by a MF-5D Fluxmeter from Walker Scientific. The Fluxmeter integrates the voltage from the pick-up coil to calculate flux density which is sent via an analog output to the Quattro data acquisition device. This process of calculating the flux density is shown in the following equations,

$$B = \frac{\phi}{A} = \mu_o \mu_r H, \quad (3.1)$$

$$V = -N \frac{d\phi}{dt}, \quad (3.2)$$

$$B = -\frac{1}{NA} \int V dt. \quad (3.3)$$

The flux density flowing through the test sample is equivalent to the flux divided by the area of the sample (Eq 3.1). The pick-up coil placed at the center of test sample produces a voltage proportional to the change in flux (Eq 3.2). Therefore, the flux density through the test sample can be measured by integrating the pick-up coil voltage with respect to time (Eq 3.3). The Fluxmeter integrates the pick-up coil voltage, but the Fluxmeter must be calibrated to the pick-up coil used. Therefore, the $1/NA$ term needs to be found for the

pick-up coil. To determine this, a Nickel 200 sample 0.25 inches in diameter was placed in the magnetomechanical transducer and the quasi static response was measured. The $1/NA$ input to the Fluxmeter was changed until the experimental magnetization curves, Figure 16, matched previously measured magnetization curves for Nickel 200 conducted by Smith et al., Figure 17 [12]. The Fluxmeter was calibrated to have a setting of 23 cm^2 to correspond to the NA term. From the area and number of turns of the pick-up coil, the actual NA value is 23.46 cm^2 . A 1.9% difference between the calibrated NA value and the actual value helps validate the calibration of the Fluxmeter.

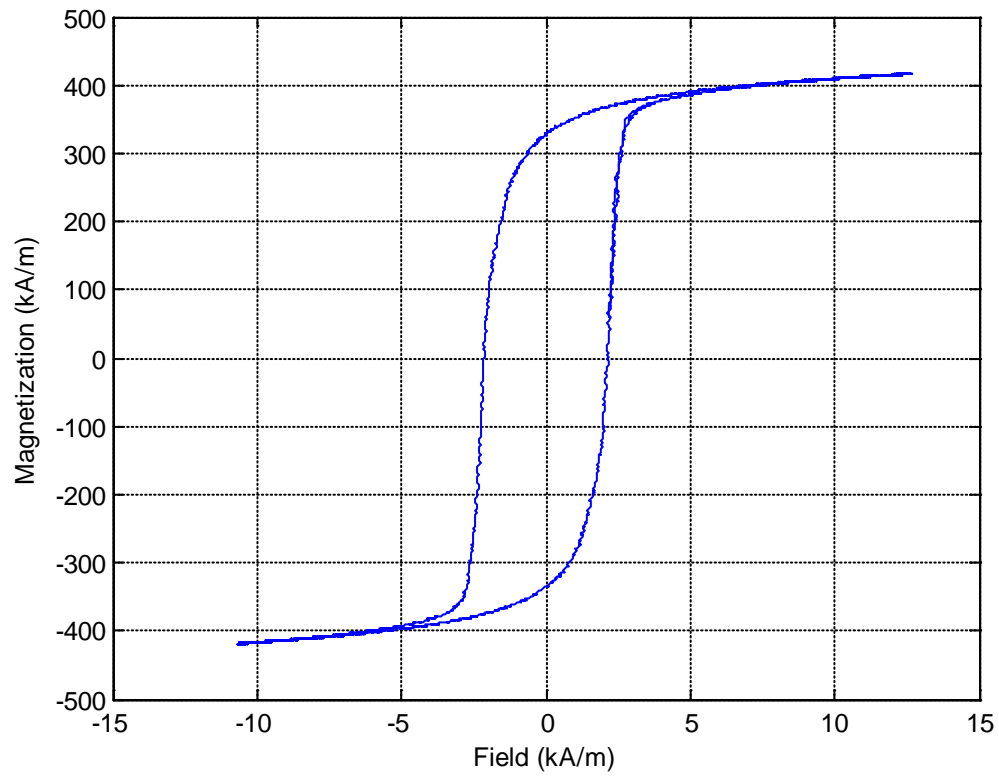


Figure 16: Magnetization curves of Nickel 200 in the magnetomechanical transducer used to calibrate the MF-5D Fluxmeter for future testing.

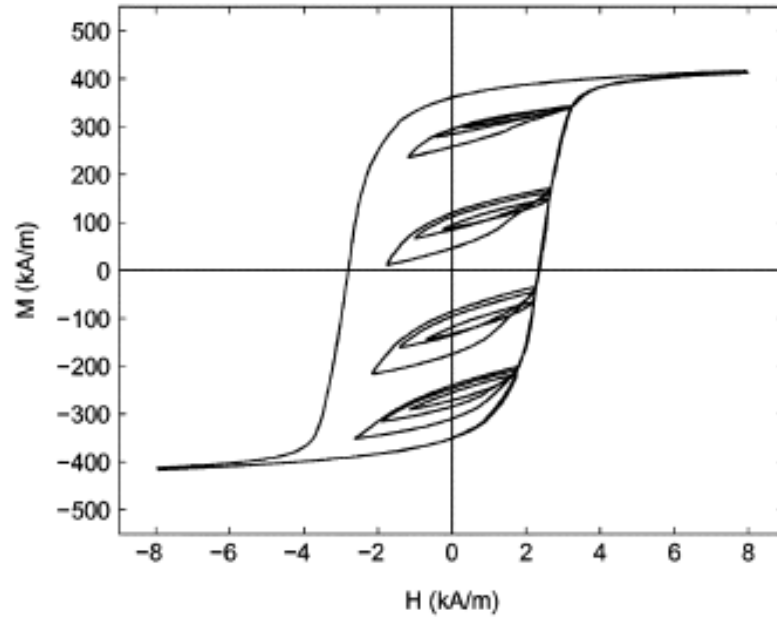


Figure 17: Magnetization curves of Nickel 200 measured experimentally [12].

CHAPTER 4

RESULTS AND ANALYSIS

In this section the magnetomechanical transducer constructed and measurement system developed are used to measure the response of Galfenol samples. Quasi static actuation measurements are conducted to validate the functionality of the transducer. A physical model of a Galfenol rod with a mass load subjected to an actuation test is created. The goal of the project is to assist in characterizing the dynamic behavior of Galfenol. Therefore, dynamic actuation tests are conducted and analyzed to initiate dynamic characterization.

4.1 Quasi static actuation test

The purpose of this test was to validate the magnetomechanical transducer and measurement system. The $\text{Fe}_{81.6}\text{Ga}_{18.4}$ sample was measured both with no load and a mass load (Figure 12b). A mass load of 50 lbs, 7 MPa, was applied for that respective test. A sinusoidal input at 100 mHz was applied to the system. Results of the test are shown in Figure 18. The data from the tests validates the functionality of the transducer and the effectiveness of the measurement system.

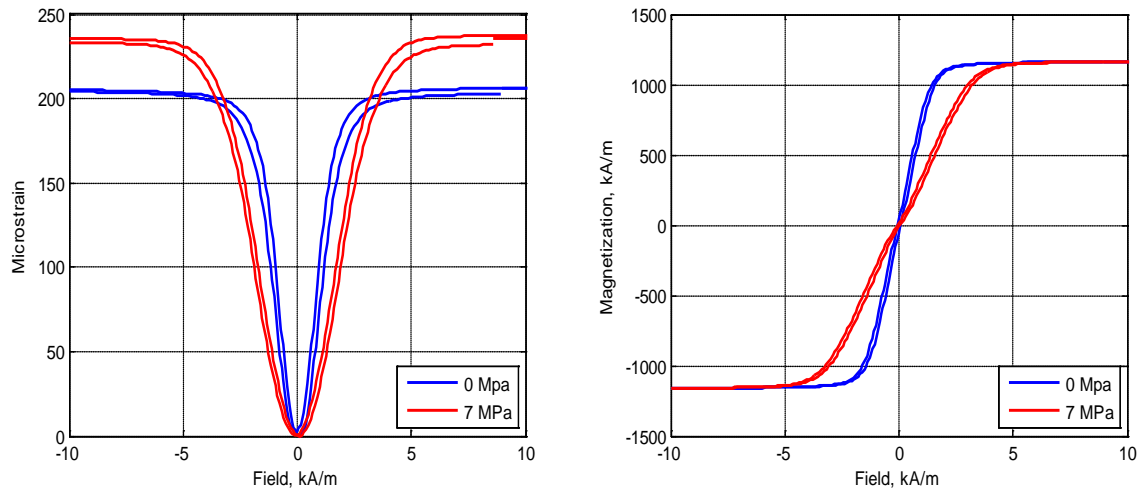


Figure 18: Quasi static actuation measurements of $\text{Fe}_{81.6}\text{Ga}_{18.4}$ sample conducted at 100 mHz.

4.2 Mechanical model

A single degree of freedom mechanical model of a Galfenol sample subjected to a sinusoidal magnetic input was developed to give an estimate of the resonant frequency at various loads. The sample is fixed at one end and coupled to a mass load at the other. A schematic of the model and a free body diagram of the system are shown in Figure 19. The magnetic input creates a force in the Galfenol sample related to the elastic modulus, area, and magnetostriction as a function of field. This sinusoidal force acts on the spring-mass-damper model of the Galfenol sample and mass load. The equivalent mass is calculated by the following equation [11],

$$m_{eq} = \frac{m}{3} + M, \quad (4.1)$$

where m is the mass of Galfenol sample and M is the mass of the load. The Galfenol sample acts as a spring with a spring constant $k = EA/l$.

The damping of the system was not measured, and it was assumed that the system was underdamped. A damping constant c value of 0.02% of the spring constant was used. Assuming a damping constant this small, the resonant frequency is mostly dependent on the equivalent mass and effective spring constant of the system. The response of the model at varying frequencies is given by the following transfer function,

$$TF = \frac{F}{m_{eq}\omega^2 + c\omega + k}. \quad (4.2)$$

The frequency response of the model with varying loads are shown in Figure 20. The magnitude of the response is normalized such that the magnitude at 100 Hz is 0 dB.

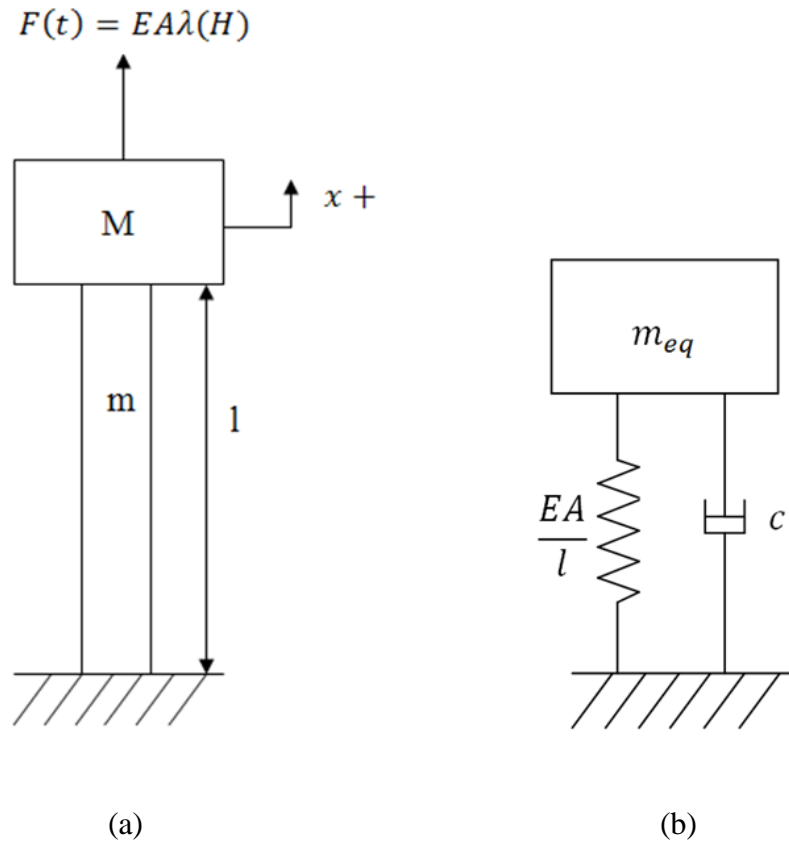


Figure 19: (a) Single degree of freedom mechanical model of Galfenol sample, m , subjected to a sinusoidal magnetic input, H , and (b) a free body diagram of the equivalent system.

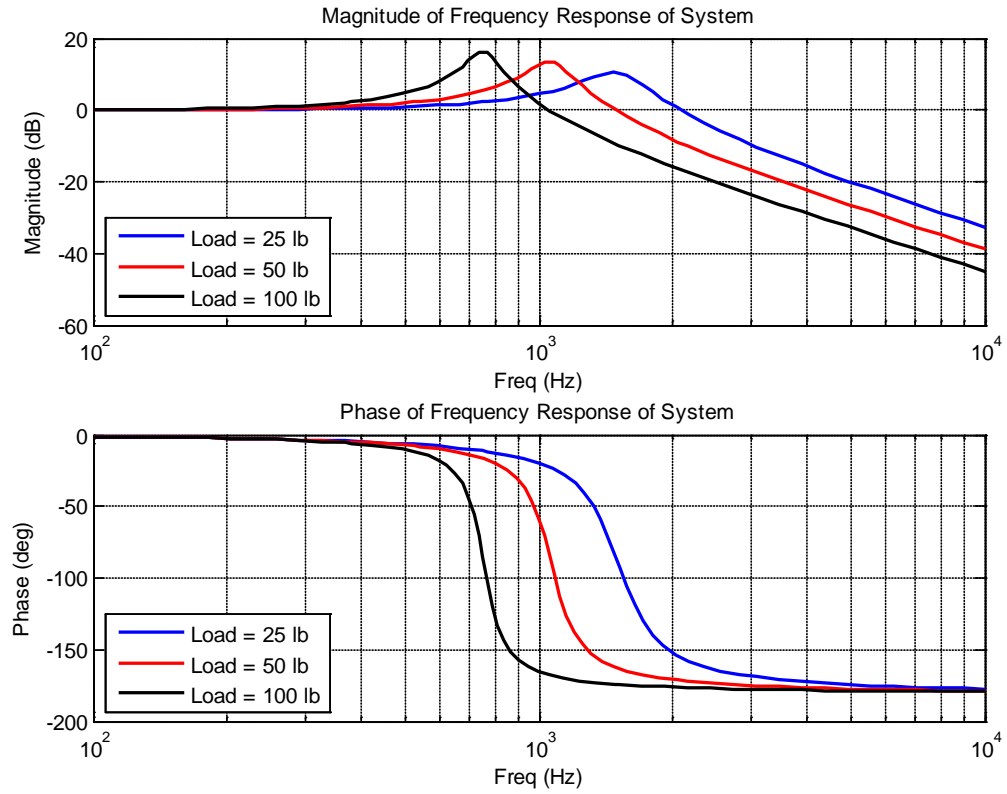


Figure 20: Frequency response of single degree of freedom mechanical model of Galfenol sample subjected to a sinusoidal magnetic input. The magnitude of the response is normalized such that the magnitude at 100 Hz is 0 dB.

4.3 Dynamic actuation tests

Dynamic actuation tests were conducted with the $\text{Fe}_{81.6}\text{Ga}_{18.4}$ sample. The sample was subjected to a 50 lb mass load. The tests were conducted over the frequency span of 1 Hz to 500 Hz. The input to the system had a magnetic bias of 2 kA/m and an amplitude of 1 kA/m. The λ -H and M-H curves of the tests are shown in Figure 21 and Figure 22. The magnetostriction at each frequency is normalized such that the minimum value is zero. Based on quasi static data, the magnetization values were normalized so that $M = 420$ kA/m when $H = 2$ kA/m at 1 Hz. Additional detail of tests can be seen in Appendix A and Appendix B including time domain plots and signal filtering.

From these measurements, the piezomagnetic constant, d , and the susceptibility, $(\mu-1)$, were calculated from the following equations [14],

$$d = \frac{dS}{dH}, \quad (4.3)$$

$$(\mu - 1) = \frac{dM}{dH}, \quad (4.4)$$

The values were calculated using numerical differentiation at fields of 1.3-2.7 kA/m. The entire field range of 1-3 kA/m was not used to avoid differentiating at the limits of the measurements resulting in values approaching infinity. The resulting data was then filtered by using a moving average. Results of these calculations at each frequency are shown below in Figure 23 and Figure 24.

The results of the tests show that the hysteresis in the system expands as the frequency increases. Additionally, the phase of the λ -H and M-H curves increases with increasing frequency. The d-H and $(\mu-1)$ -H curves show symmetry about the biased field point of 2 kA/m. Susceptibility measurements at low frequencies are not symmetric due to kinking at low fields which can be seen in the static measurements (Figure 18).

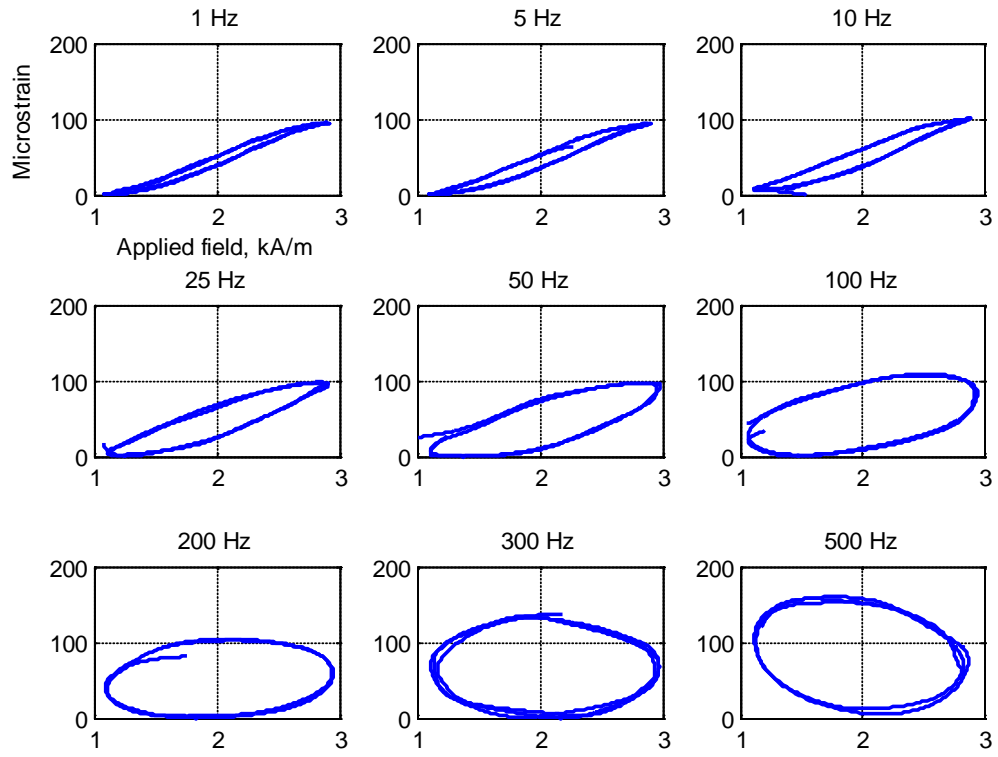


Figure 21: Magnetostriction-field curves for actuation measurements of $\text{Fe}_{81.6}\text{Ga}_{18.4}$ sample with a mass load of 50 lb at 1, 5, 10, 25, 50, 100, 200, 300, and 500 Hz. The minimum magnetostriction value was normalized to zero for each test.

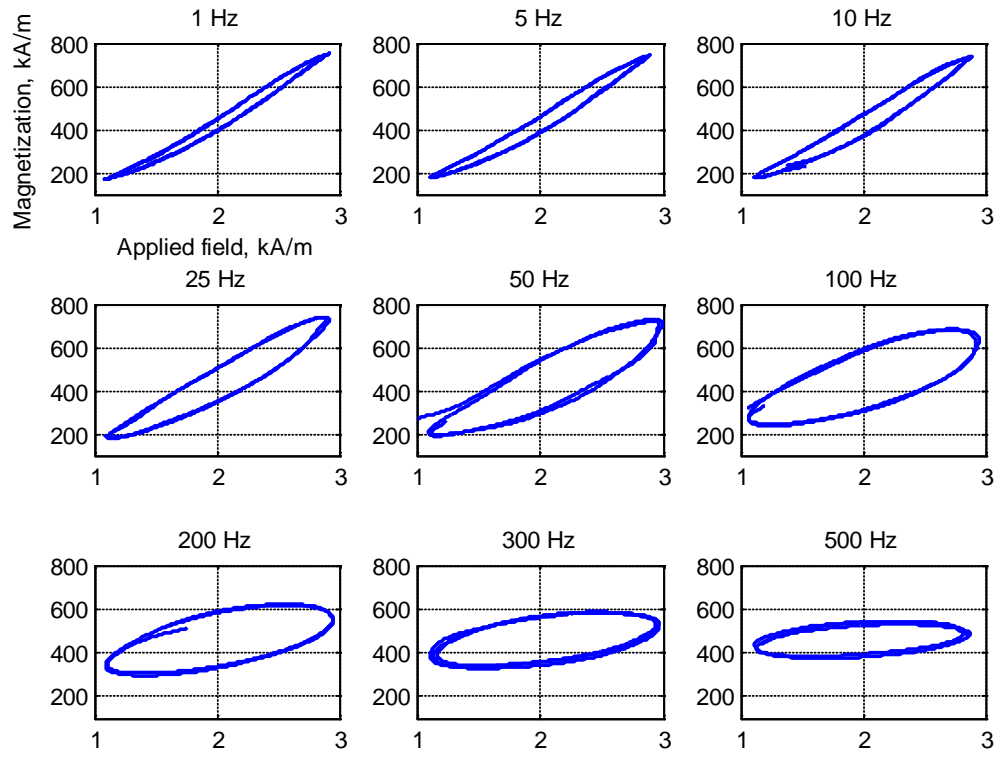


Figure 22: Magnetization-field curves for actuation measurements of $\text{Fe}_{81.6}\text{Ga}_{18.4}$ sample with a mass load of 50 lb at 1, 5, 10, 25, 50, 100, 200, 300, and 500 Hz. Magnetization values are normalized such that $M = 420$ kA/m at $H = 2$ kA/m at 1 Hz.

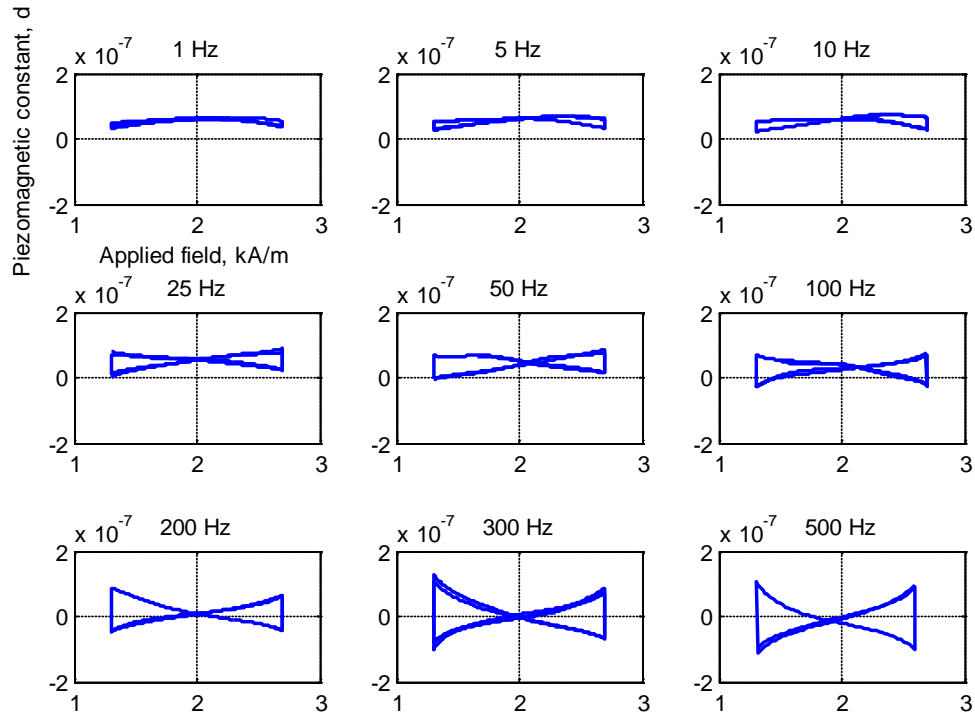


Figure 23: Piezomagnetic constant, d , versus magnetic field for actuating measurements of $\text{Fe}_{81.6}\text{Ga}_{18.4}$ sample with a mass load of 50 lb at 1, 5, 10, 25, 50, 100, 200, 300, and 500 Hz. The values of d were calculated using numerical differentiation and filtered using a moving average. Values were calculated from $H = 1.3\text{--}2.7$ kA/m to avoid differentiation at the limits of the measurements.

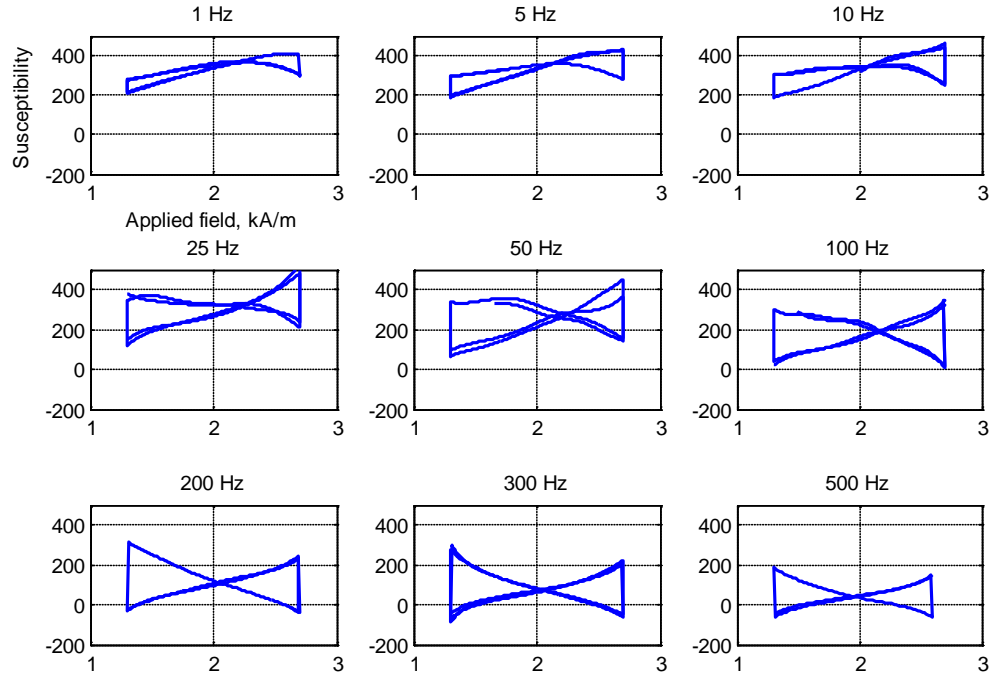


Figure 24: Susceptibility, ($\mu-1$), versus magnetic field for actuating measurements of $\text{Fe}_{81.6}\text{Ga}_{18.4}$ sample with a mass load of 50 lb at 1, 5, 10, 25, 50, 100, 200, 300, and 500 Hz. Susceptibility values were calculated using numerical differentiation and filtered using a moving average. Values were calculated from $H = 1.3\text{-}2.7$ kA/m to avoid differentiation at the limits of the measurements.

CHAPTER 5

SUMMARY AND CONCLUSIONS

In this thesis, the dynamic characterization of Galfenol alloys has been investigated. First, a magnetomechanical transducer was designed and constructed for actuation and sensing measurements of a research grade, highly textured, $\langle 100 \rangle$ oriented polycrystalline Galfenol alloy with the composition $\text{Fe}_{81.6}\text{Ga}_{18.4}$. This transducer was designed to produce uniform magnetic field and strain along the length of the test samples. The finished transducer utilized two excitation coils connected to a closed magnetic flux path. Flux created by the coils flowed through the path and into the Galfenol test sample. The transducer was successfully constructed and its functionality was validated through quasi static actuation tests.

The measurement system associated with the magnetomechanical transducer was developed. The system measured electrical, mechanical, and magnetic parameters necessary for characterizing the Galfenol samples under both static and dynamic testing conditions. This measurement system was used to conduct quasi static tests verifying the transducer's effectiveness. Also, it was used to conduct dynamic actuation tests up to

500 Hz. These dynamic actuation tests revealed increasing hysteresis and phase at higher frequencies.

This project was a successful first step towards characterizing Galfenol under dynamic conditions. Further work needs to be done to gather more experimental data using Galfenol as both an actuator and sensor. A comprehensive set of experiments at varying parameters will help determine optimal conditions of the material for specific applications. A comprehensive dynamic characterization will be a great advancement in the knowledge of Galfenol alloys.

BIBLIOGRAPHY

- [1] J. Atulasimha. Characterization and Modeling of the Magnetomechanical Behavior of Iron-Gallium Alloys. *Ph.D. Dissertation, University of Maryland*. College Park, Maryland. 2006.
- [2] F. T. Calkins, M. J. Dapino, and A. B. Flatau. Overview of Magnetostrictive Sensor Technology. *Journal of Intelligent Material Systems and Structures*, 18, 2007.
- [3] F. T. Calkins, M. J. Dapino, and A. B. Flatau. Effect of prestress on the dynamic performance of a Terfenol-D transducer. *SPIE Smart Materials and Structures Symposium*, 1997.
- [4] M. J. Dapino. Magnetostrictive Materials. Ed. M. Schwartz. New York: John Wiley & Sons, Inc. 2002.
- [5] M. J. Dapino, A. B. Flatau, and F. T. Calkins. Statistical Analysis of Terfenol-D Material Properties. *Journal of Intelligent Material Systems and Structures*, 17: 587-599, 2006.
- [6] P. G. Evans. Nonlinear Magnetomechanical Modeling and Characterization of Galfenol and System-Level Modeling of Galfenol-Based Transducers. *Ph.D. Dissertation, The Ohio State University*. Columbus, Ohio. 2009.
- [7] P. G. Evans. State-Space Constitutive Model for Magnetization and Magnetostriction of Galfenol Alloys. *IEEE Transactions on Magnetics*, 44 (7), 2008.
- [8] P. G. Evans and M. J. Dapino. Fully-coupled magnetoelastic model for Galfenol alloys incorporating eddy current losses and thermal relaxation. *Proceedings of SPIE*, 6929, 2008.
- [9] P. G. Evans and M. J. Dapino. Measurement and Modeling of Magnetomechanical Coupling in Magnetostrictive Iron-Gallium Alloys. *SPIE Smart Materials and Structures Symposium*, 2009.
- [10] R. A. Kellogg, A. Flatau, A. E. Clark, M. Wun-Fogle, and T. Lograsso. Quasi-static Transduction Characterization of Galfenol. *Journal of Intelligent Material Systems and Structures*, 16:471-479. 2005.

- [11] Rao, S. S. *Mechanical Vibrations* (4th ed.). Upper Saddle River: Pearson Prentice Hall. 2004.
- [12] R. C. Smith, M. J. Dapino, M. J. Braun, and A. P. Mortensen. A Homogenized Energy Framework for Ferromagnetic Hysteresis. *IEEE Transactions on Magnetics*, 42 (7). 2006.
- [13] L. M. Twarek and A. B. Flatau. Dynamic property determination of magnetostrictive iron-gallium alloys. *Smart Structures and Materials 2005: Active Materials: Behavior and Mechanics*. 2005.
- [14] M. Wun-Fogle, J. B. Restorff, and A. E. Clark. Magnetomechanical Coupling in Stress-Annealed Fe-Ga (Galfenol) Alloys. *IEEE Transactions on Magnetics*, 42 (10). 2006.

APPENDIX

Appendix A: Time domain plots of actuation tests

Dynamic actuation tests were conducted with the $\text{Fe}_{81.6}\text{Ga}_{18.4}$ sample and were detailed in Section 4.3. Time domain plots of field, magnetization, and strain at each frequency are shown below. The signals shown have been filtered using an iterative moving average which is discussed in Appendix B.

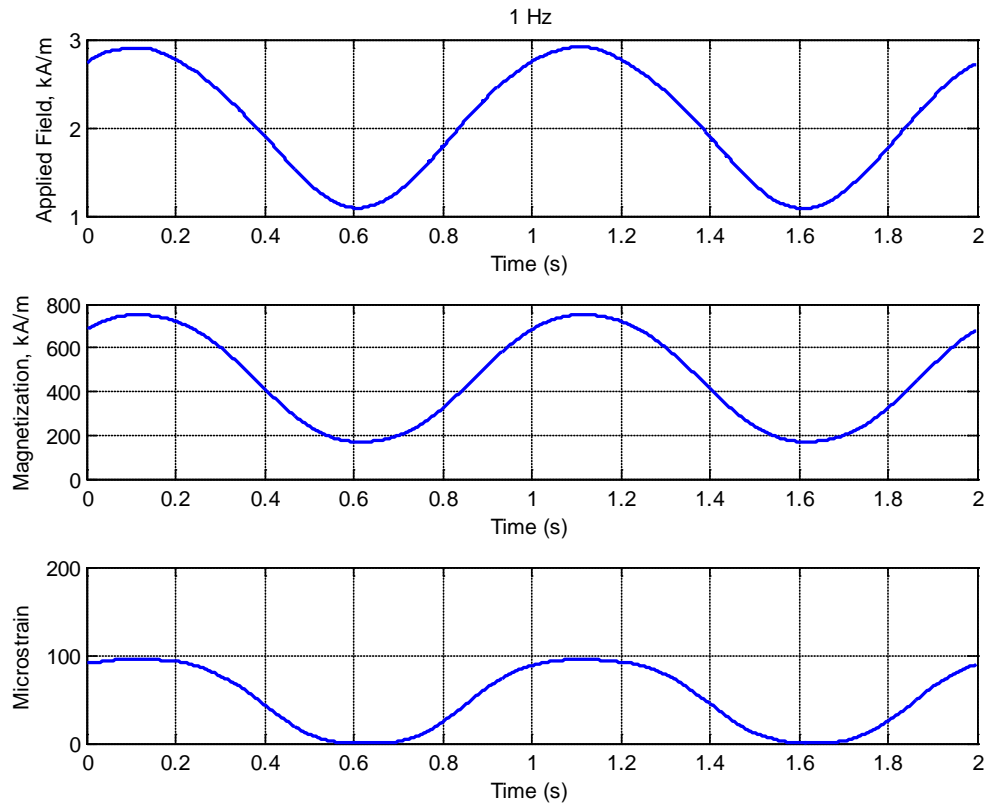


Figure A1: Time domain plot of actuation test at 1 Hz showing (i) applied field, (ii) magnetization, and (iii) strain.

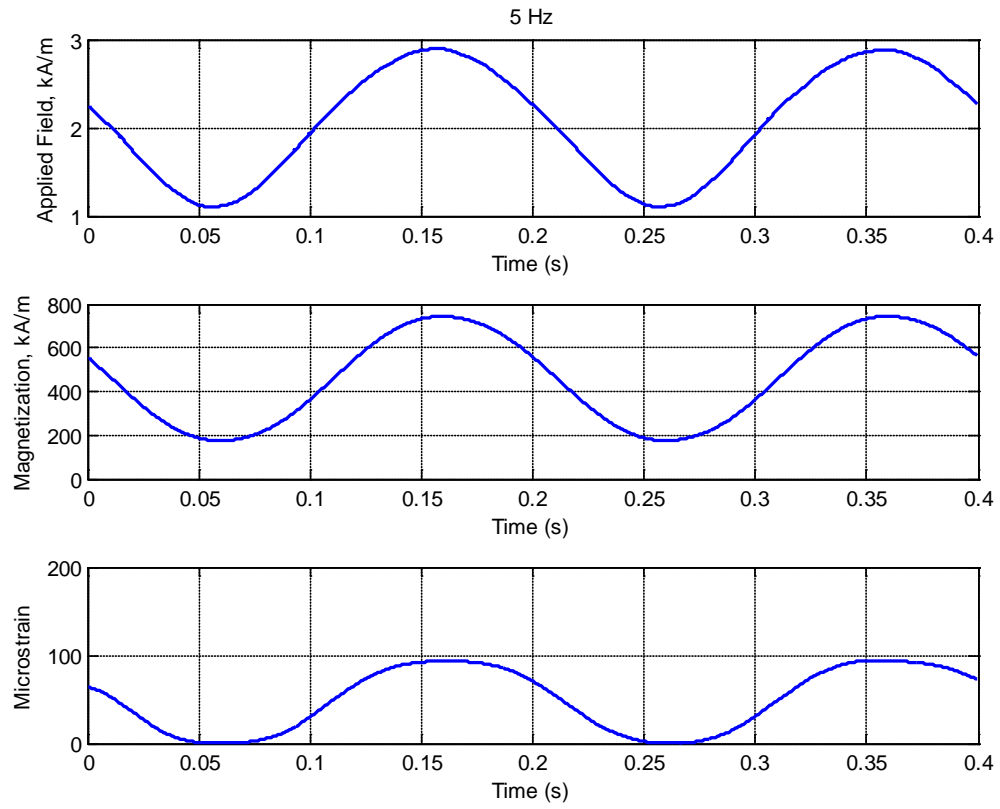


Figure A2: Time domain plot of actuation test at 5 Hz showing (i) applied field, (ii) magnetization, and (iii) strain.

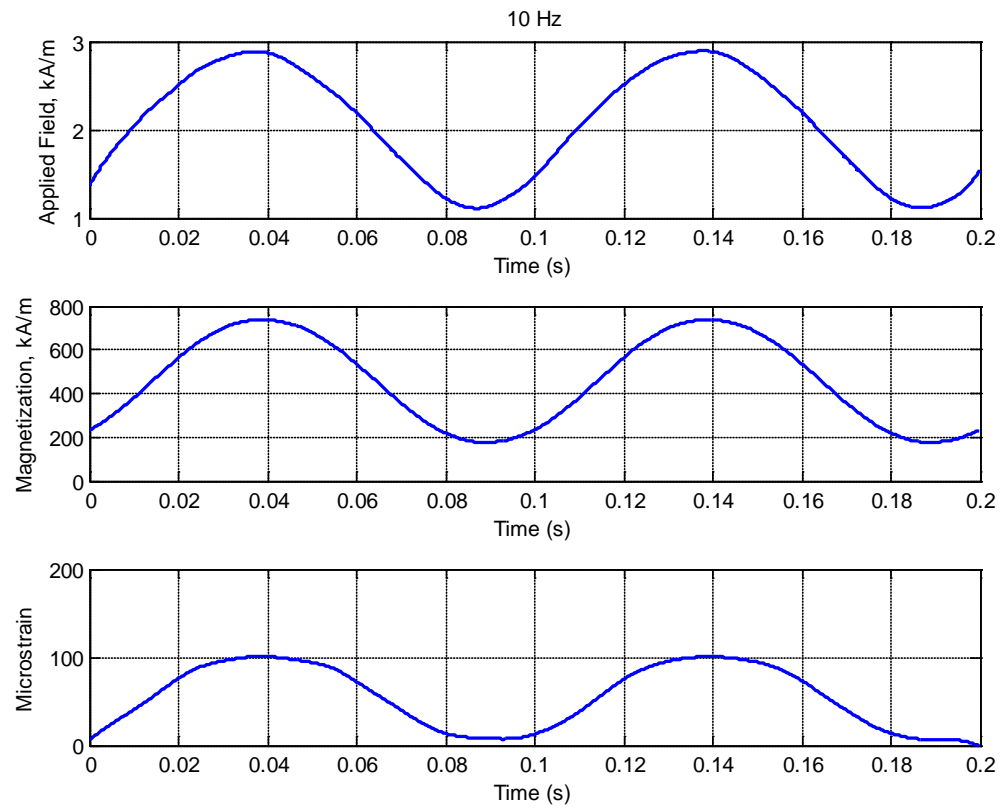


Figure A3: Time domain plot of actuation test at 10 Hz showing (i) applied field, (ii) magnetization, and (iii) strain.

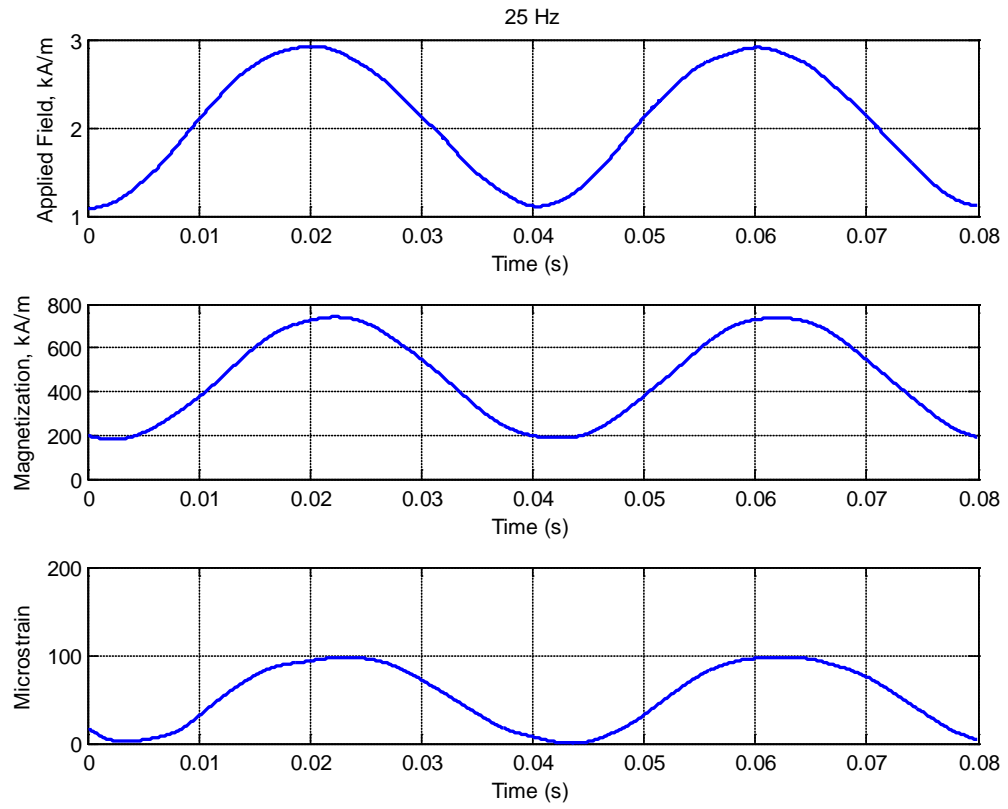


Figure A4: Time domain plot of actuation test at 25 Hz showing (i) applied field, (ii) magnetization, and (iii) strain.

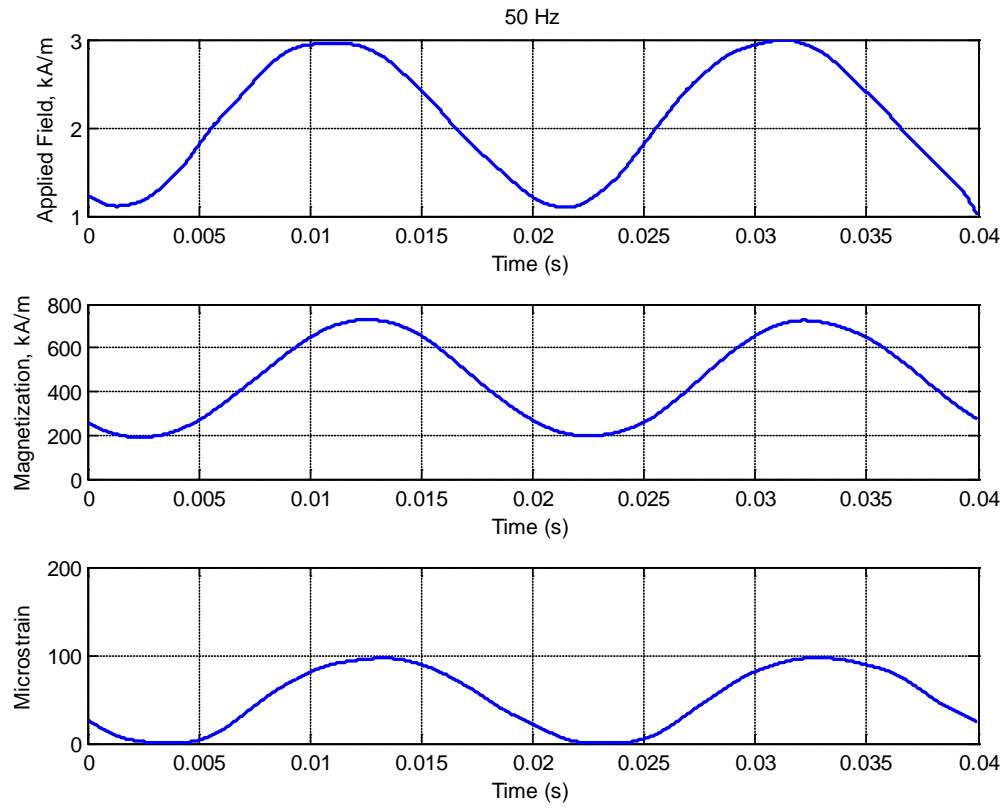


Figure A5: Time domain plot of actuation test at 50 Hz showing (i) applied field, (ii) magnetization, and (iii) strain.

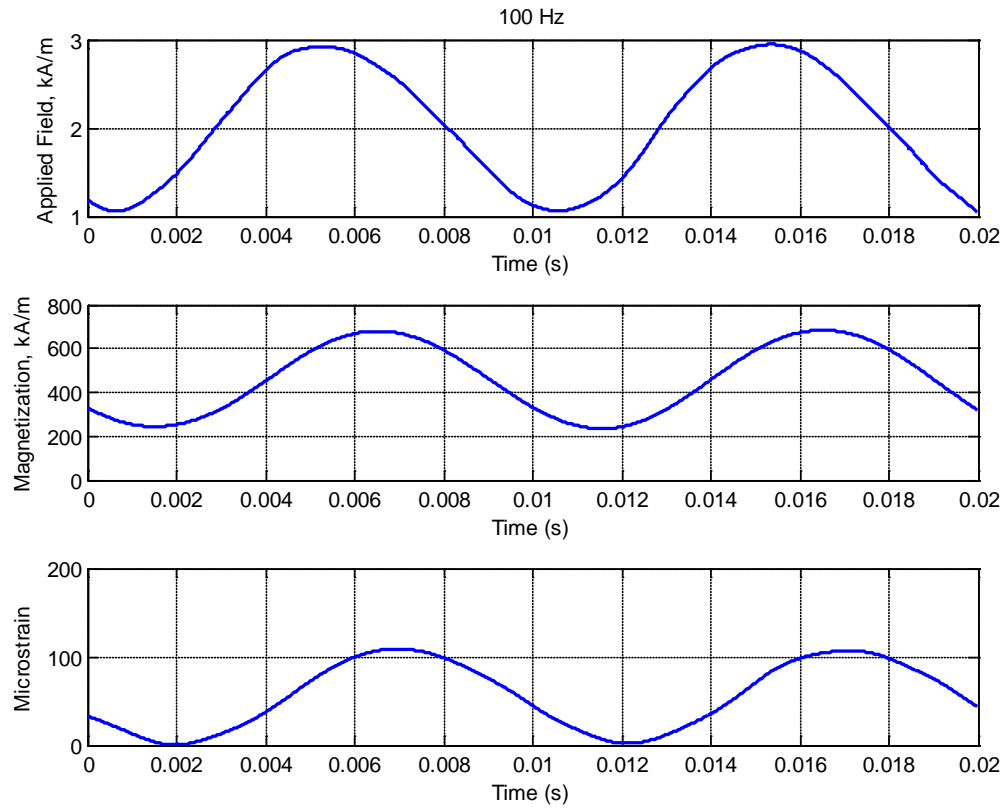


Figure A6: Time domain plot of actuation test at 100 Hz showing (i) applied field, (ii) magnetization, and (iii) strain.

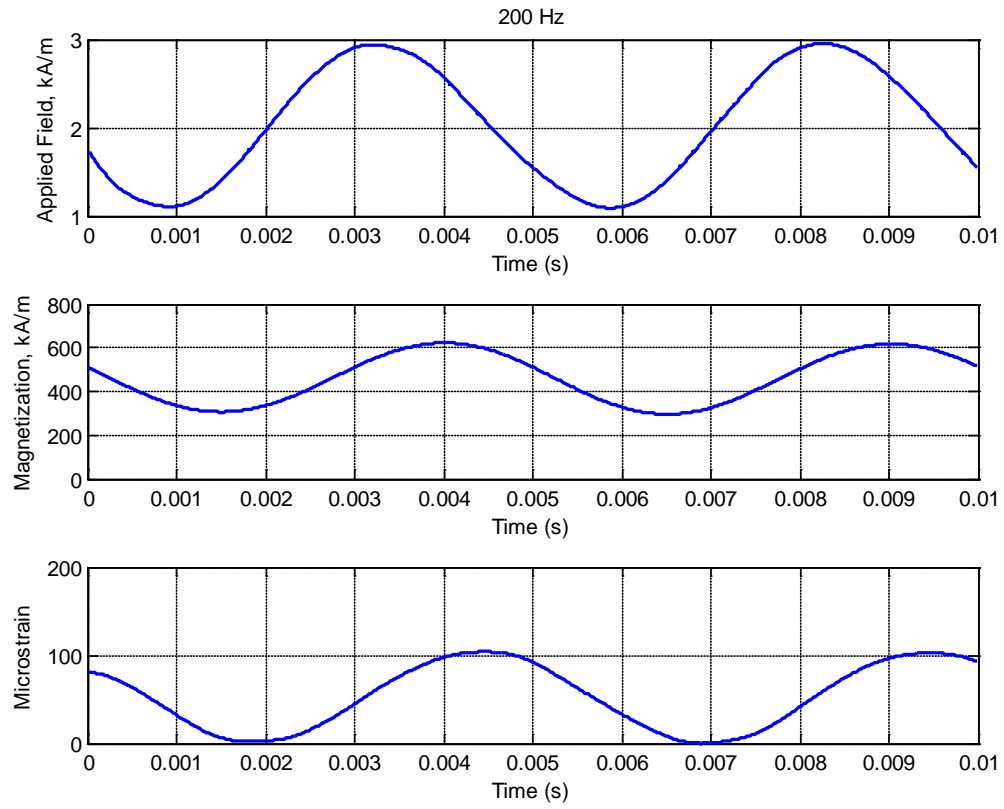


Figure A7: Time domain plot of actuation test at 200 Hz showing (i) applied field, (ii) magnetization, and (iii) strain.

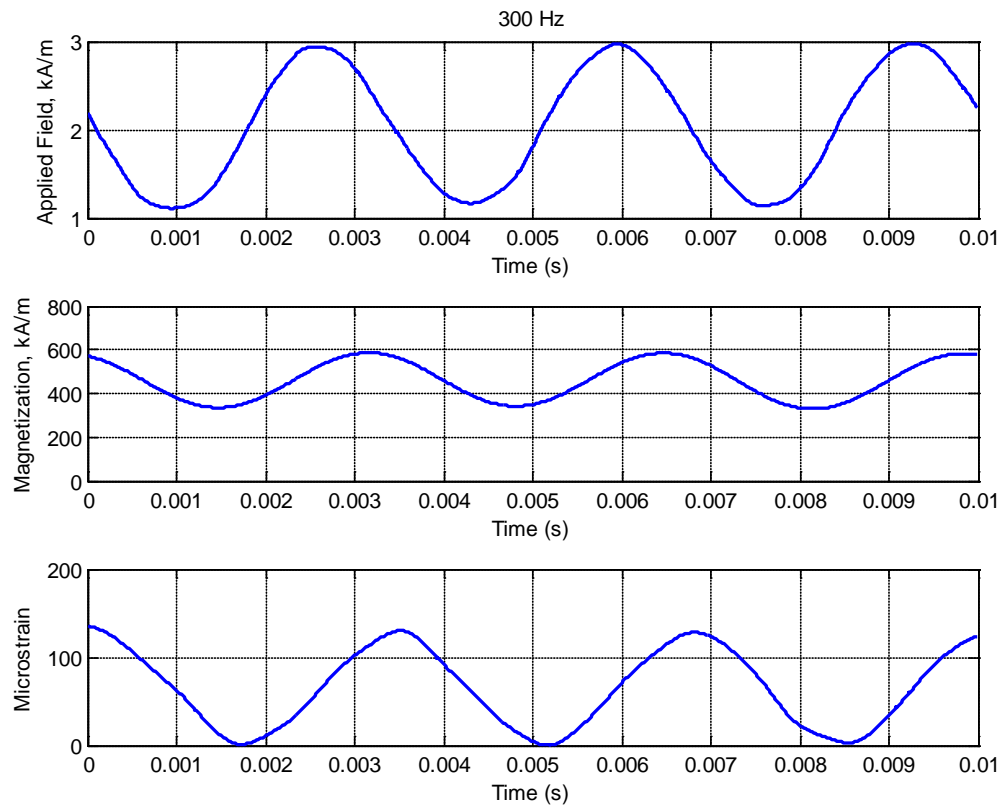


Figure A8: Time domain plot of actuation test at 300 Hz showing (i) applied field, (ii) magnetization, and (iii) strain.

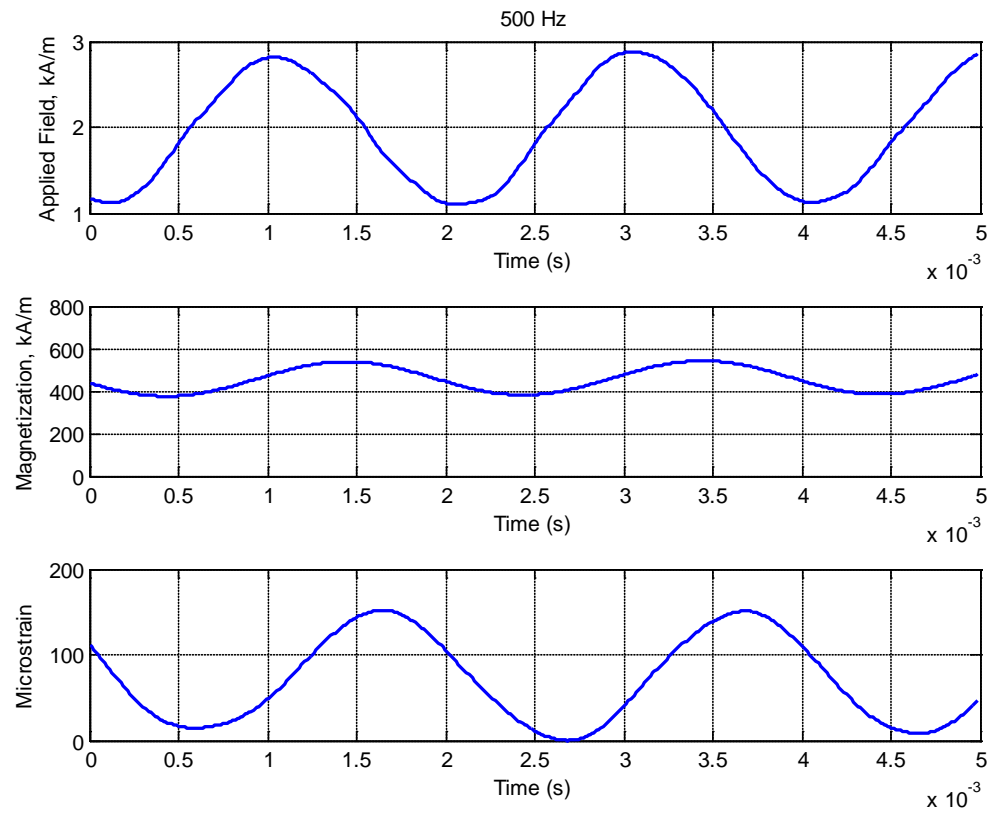


Figure A9: Time domain plot of actuation test at 500 Hz showing (i) applied field, (ii) magnetization, and (iii) strain.

Appendix B: Signal filtering in actuation tests

The measurements shown for the actuation tests in Section 4.3 were filtered. To reduce noise in the field and strain measurements, a moving average filter was applied to each in MATLAB. An iterative process was used to filter the signals as applying the moving average once was not sufficient to decrease the noise to an acceptable level. The parameters of the moving average and number of iterations were optimized at each frequency to ensure that the filtered signal closely matched the measured signal. Comparisons of the original signal and the filtered signal at different amounts of iteration for the 25 Hz test are shown below. Figure B1 and Figure B2 show that the moving average filter is ineffective if not used with enough iterations. Figure B3 compares the original and filtered signal at the accepted parameters used to filter the signal at 25 Hz.

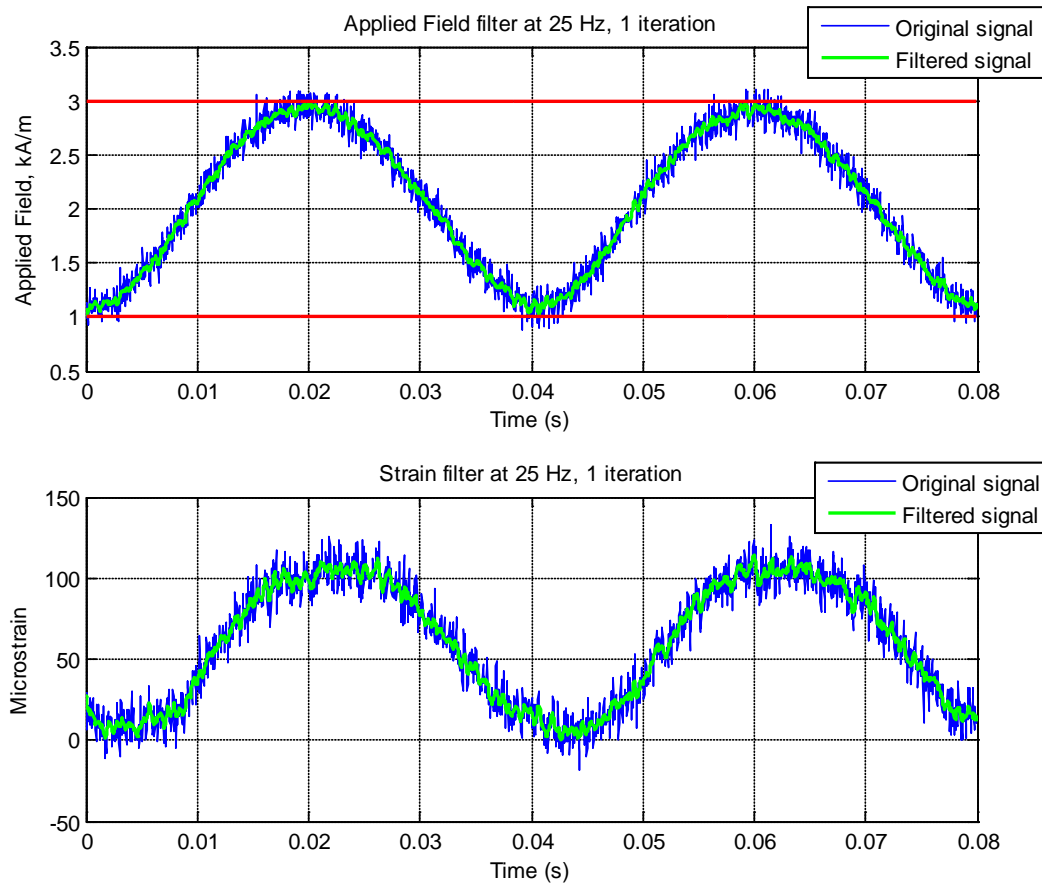


Figure B1: Comparison of the original and filtered signals for (i) applied field and (ii) strain of an actuation test at 25 Hz. One iteration of the moving average filter was applied.

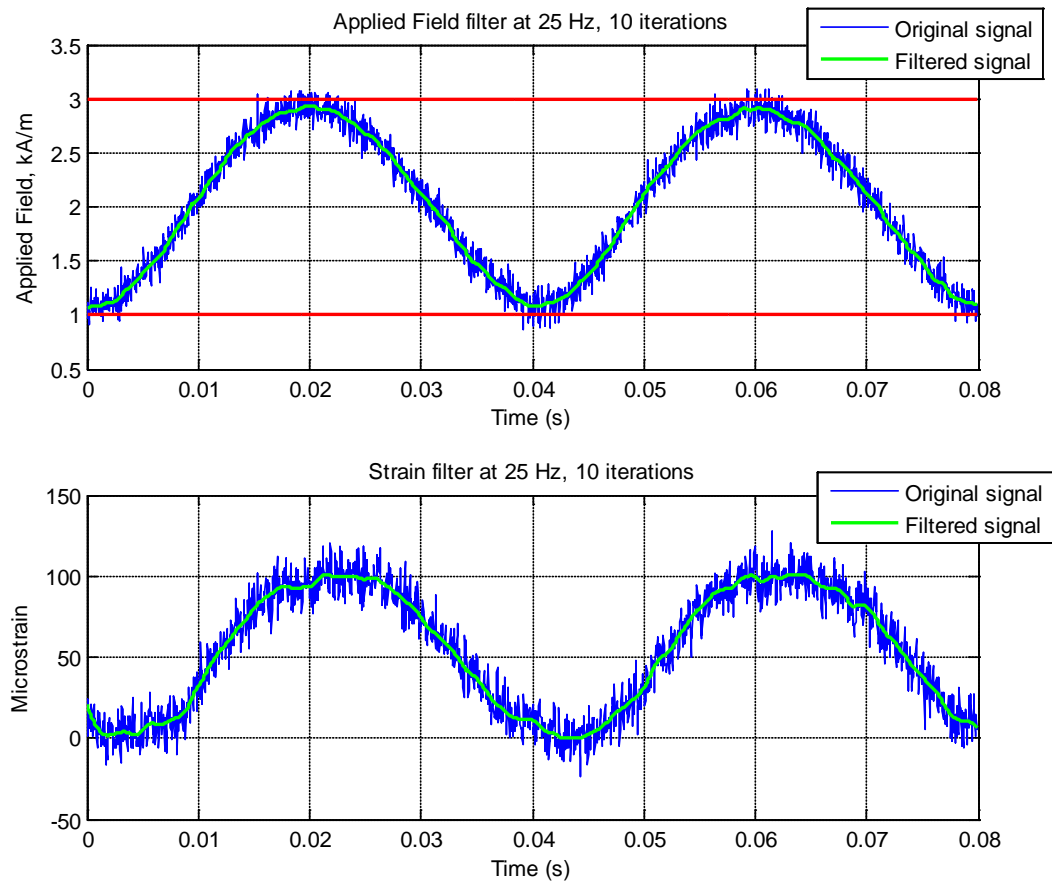


Figure B2: Comparison of the original and filtered signals for (i) applied field and (ii) strain of an actuation test at 25 Hz. Ten iterations of the moving average filter were applied.

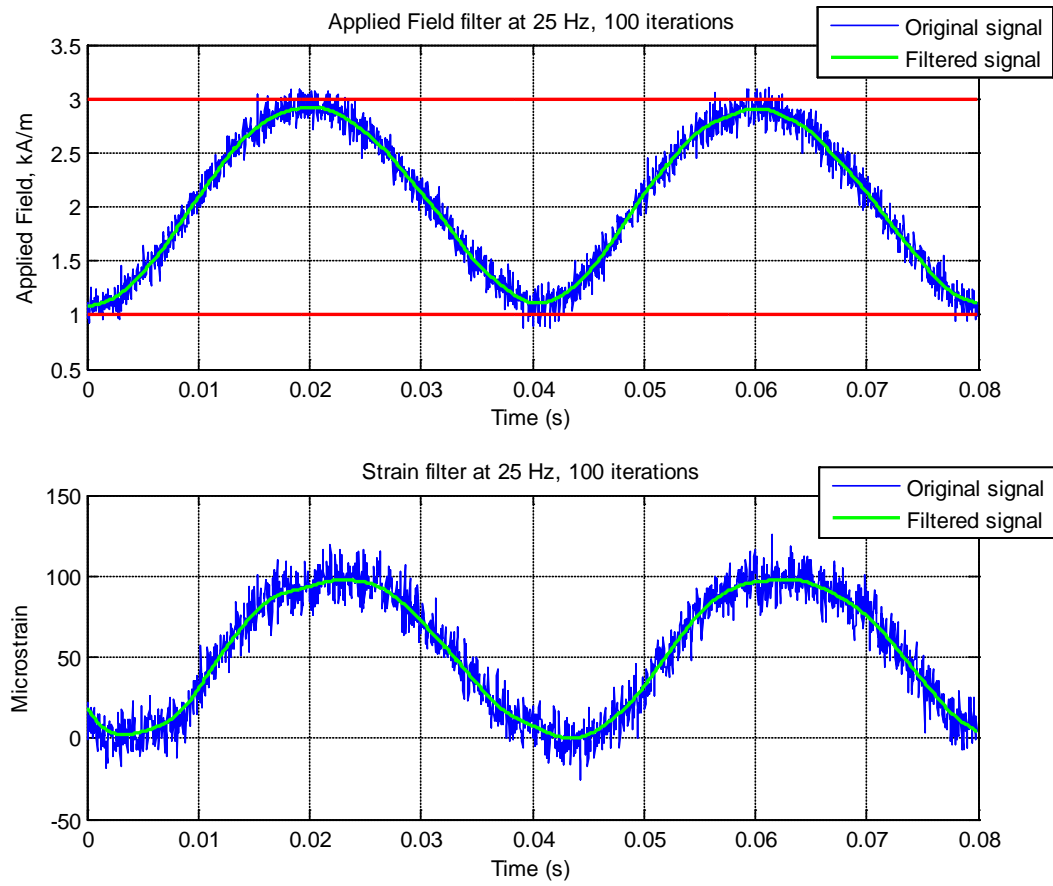


Figure B3: Comparison of the original and filtered signals for (i) applied field and (ii) strain of an actuation test at 25 Hz. One hundred iterations of the moving average filter were applied.